

**POLYTECHNIC UNIVERSITY OF BUCHAREST  
FACULTY OF INDUSTRIAL AND ROBOTIC ENGINEERING**



**THESIS**

**INNOVATIVE DESIGN AND MANUFACTURING  
METHOD OF A NEW PRODUCT**

**METODĂ INOVATIVĂ DE CONCEPȚIE ȘI  
REALIZARE A UNUI PRODUS NOU**

**Author:**

**SUVAC Albert Mihai**

**Scientific leader:**

**Prof. Dr. Eng. COTEȚ Costel Emil**

**DOCTORAL COMMISSION**

Chairman	Prof. univ. dr. ing. Adrian Florin Nicolescu	de la	Universitatea Politehnica din București
Scientific leader	Prof. univ. dr. ing. Costel Emil COTEȚ	de la	Universitatea Politehnica din București
Reviewer	Prof. univ. dr. ing. George Emilian Drăghici	de la	Universitatea Politehnica Timișoara
Reviewer	Prof. univ. dr. ing. Paul-Dan BRINDASU	de la	Universitatea „Lucian Blaga” din Sibiu
Reviewer	Prof. univ. dr. ing. Miron ZAPCIU	de la	Universitatea Politehnica din București

**Bucharest  
2020**

## Innovative design and manufacturing method of a new product



## content

### Introduction 7

<b>Chapter 1.</b> Instrumentalization of the life cycle for the conception and realization of a new product	8
<b>Chapter 2.</b> Brief study on the method. ....	9
<b>Chapter 3.</b> Innovative elements assumed through the objectives and structure of the thesis starting from existing methods and solutions.....	11
3.1. The objectives of the doctoral thesis .....	13
3.2. The structure of the doctoral thesis and the topics addressed in each chapter .....	13
3.3. Performance and limitations of current technical solutions. Characteristics of the electric vehicle case study .....	14
3.4. Limitations of existing products on the market .....	20
<b>Chapter 4.</b> Manufacturing methods and technologies for metal structures used in the construction of the new product.....	22
<b>Chapter 5.</b> Presentation of the innovative method of design and production of a new product for an electric vehicle case study .....	25
5.1. The new product design method.....	25
5.2. Presentation of the evolutionary design algorithm in five stages for the new product	25
5.2.1. Stage I .....	25
5.2.2. Stage II.....	36
5.2.3. Stage III.....	37
5.2.4. Stage IV .....	41
5.2.5. Stage V.....	42
<b>Chapter 6.</b> Experimental determinations for the validation of the innovative five-stage design algorithm	43
6.1. Analysis of the behavior of the steel frame using the finite element method .....	44
6.2. Finite element analysis of the aluminum frame.....	44
6.3. Research on the determination of displacements using tensometric transducers .....	45
6.4. Measuring the stiffness of the steel arm .....	46
6.5. Measurements with tensometric transducers on the steel rear axle arm, with elastic damping system .....	48
6.6. Measurements with tensometric transducers on the steel rear axle arm, with elastic damping system .....	48
6.7. Measurements with tensometric transducers on the aluminum rear axle arm, with elastic damping system.....	50
6.8. Research on weight distribution on tricycle wheels .....	52

6.9. Measurements with resistive transducers in conditions of ascent and descent of the user	52
6.10. Dynamic study with overcoming obstacles .....	53
<b>Chapter 7. Optimization algorithms by parametric resizing of the metal structure .....</b>	<b>56</b>
7.1. Topological conceptual optimization of the framework.....	57
7.2. Theoretical optimization of the 2F1S framework.....	58
<b>Chapter 8. Conclusions, own contributions, development perspectives.....</b>	<b>63</b>
8.1. conclusions .....	63
8.2. Own contributions .....	64
8.3. Development perspectives.....	65

List of notations:

- tricycle with two front wheels and one rear wheel (2F1S)
- tricycles with one front wheel and two rear wheels. (1F2S)
- electronic control units (ECU).
- unique puncture-proof tire system (Uptis)
- product life cycle management (PLM)
- brushless DC motor (BLDC)
- carbon dioxide (CO<sub>2</sub>)
- enterprise resource planning (ERP)
- supply chain management (SCM)
- customer relationship management (CRM)
- human capital management. (HCM)
- computer aided design (CAD)
- computer aided engineering (CAE)
- computer aided manufacturing (CAM)

## **Introduction**

### **The importance of the topic of the doctoral thesis**

This doctoral thesis "Innovative method of design and realization of a new product" has as main purpose the development of an innovative model of electric tricycle, which is a viable alternative to travel in congested traffic in large urban areas. In recent years, interest in the development of mass technologies, which facilitate the mass production of small and large electric vehicles, has grown considerably. [1]. One factor that has favored this development is the facilities made available to those who want to get involved in the development of this industry in the form of state subsidies and various structural funds. [2].

Until recently, for economic reasons, the idea of sustainable development and the use of renewable energy was not a viable option for their large-scale use, especially in the automotive industry, involving high costs. [3]. Due to technological progress in recent years, the current technology available allows the development of new methods of alternative urban and rural individual transport, which would reduce carbon emissions and streamline traffic in urban areas.

The paper presents a new, topical approach to the analysis of behavior in the use of individual vehicles, trying to address their specific problems and presents innovative solutions to solve them. This is a contribution to theoretical and experimental research on manufacturing methods for the development of an innovative electric vehicle.

The developed vehicle has a design that allows folding, being easy to transport by the user, and the gauge resulting from folding allows storage in the trunk of a car or in a means of public transport.

An innovative articulation system has also been developed which gives an improved dynamic behavior of the vehicle, which increases its overall performance on uneven roads, bringing extra comfort and increased ergonomics to the user.

At the end of the paper are presented possible further developments of the individual vehicles studied and trends in manufacturing and marketing worldwide.

## Chapter 1. Instrumentalization of the life cycle for the conception and realization of a new product

Product life cycle management refers to the phasing of the entire life cycle starting from identifying the need of the product, design, analysis of design details, prototyping, execution, zero series, testing the finished product, sale, maintenance and recycling.

The definition given by professors Jörg Niemann and Engelbert Westkämper from IFStuttgart for[4] the life cycle of products is the totality of the phases of design and construction, manufacture, assembly, use, service, disassembly and recycling or renewal.

To substantiate a theoretical model of new product development based on product life cycle analysis, a complete model based on the SADT method (applied using iGrafx program 2007) developed by the team of the national research network INPRO [5]. These can be seen in Fig. 1.1.

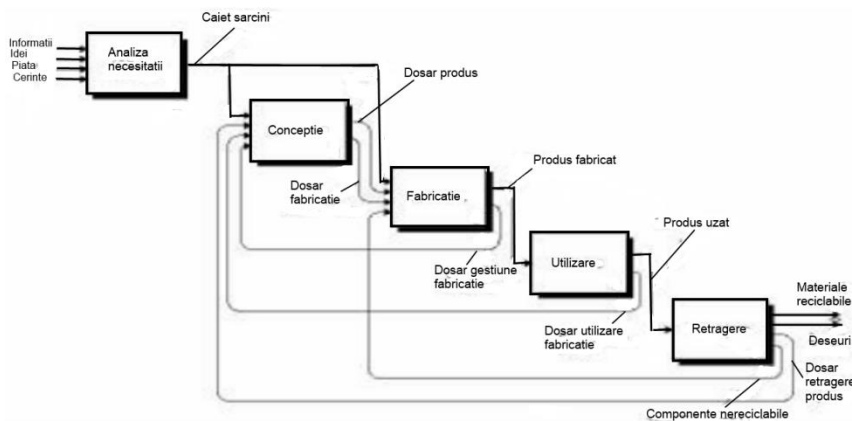


Fig. 1.1 - Diagram A0 of product life cycle activities [5]

These stages were completed for a new product dedicated to urban transport, identifying a series of particularities as follows:

- The need for the product:
- Requirements for the new product
- Ecological requirements
- Ergonomic requirements
- Aesthetic requirements
- Emotional requirements
- Economic requirements
- Design / Design
- Product design
- prototyping
- Instructions for use
- packing
- Distribution channels.
- Product maintenance
- Withdrawal
- Life cycle control model

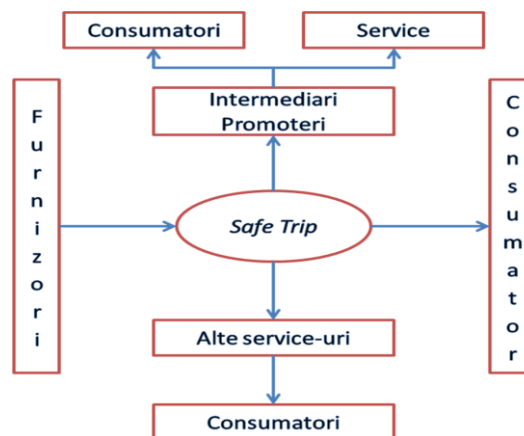


Fig. 1.2 - Distribution channels



## Chapter 2. Brief study on the method.

The growing interest in PLM can be fully explained by the advantages offered by companies in the context of a global economy: reducing the time to market a new product by reducing the time and costs associated with managing changes, capturing engineering knowledge when creating them, and the possibility of reusing information and reducing errors in the use of outdated or erroneous information, improving the product design stage and better control over projects, faster response to customer requests [6], [7], [8].

The PLM systems currently on the market (Teamcenter from Siemens, Enovia from Dassault Systemes, WindChill from PTC, Oracle Agile from Agile, SAP PLM from PLM, etc.) provide the tools and functions needed to support all the activities carried out for creating, recording, storing, retrieving and reusing information, correct and current, related to the product.

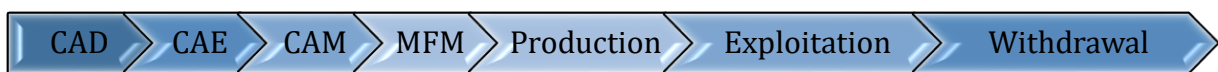


Fig. 2.1- The phases of the life cycle of a product

In the Fig. 2.1 it is a succession of the phases of the product life cycle, from the inclusion of customer requirements in the product design to the recycling of raw materials from which the product was made. We will present in detail each of these categories.

The core of the proposed method is located upstream of the Material Flow Management (MFM) module [9], [10], [11]. The method is centered around computer-aided design, engineering and manufacturing modules (CAD – Computer Aided Design, CAE – Computer Aided Engineering, CAM – Computer Aided Manufacturing). The method is based on the three modules of design, engineering and assisted manufacturing that interact with each other in a complex way. This proposed optimization method is based on the results of the SWOT analysis in Fig. 2.2. This analysis was the basis for optimizing the product based on its weaknesses. The perspectives of further development of the paper start from the SWOT analysis adapted to the different specific operating conditions stated above.

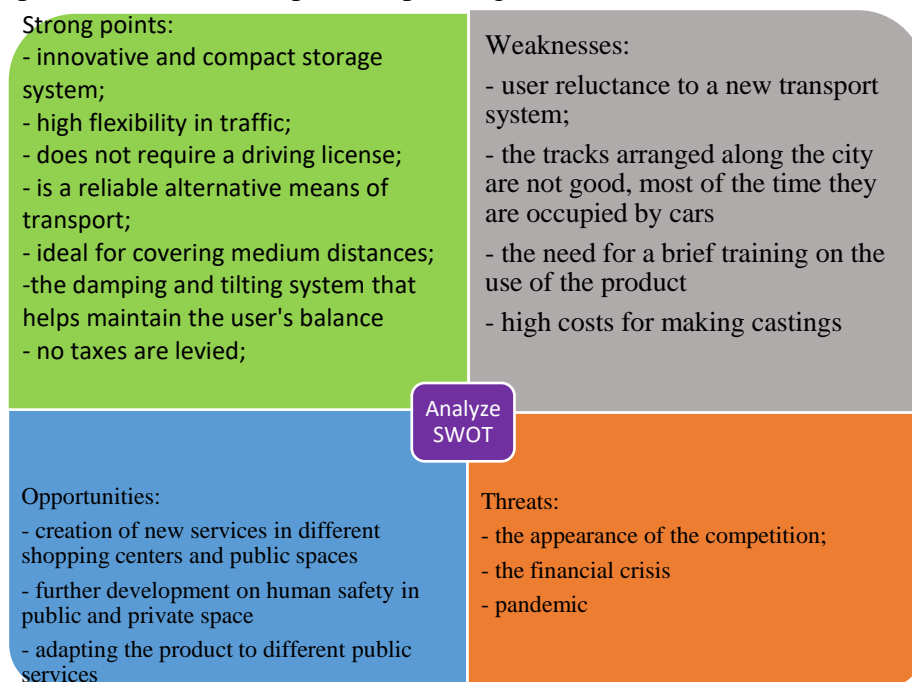
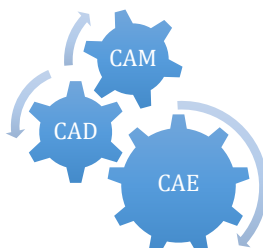


Fig. 2.2 - SWOT analysis used in the proposed method

In Fig. 2.3 shows the sequence of interactions of these first modules in PLM starting from the analysis considered above. The thesis considers in particular the interactions between the phases of assisted design for the realization of the three-dimensional virtual prototype of the product (CAD) and the simulation of its in-service behavior (CAE). If some malfunctions are identified, the product is redesigned to eliminate them. After the results of the CAE simulation become satisfactory, we move on to the next stage, the realization of the film sheet of the technological operations that we have to go through to obtain the product and the simulations of the processes associated with these operations (CAM).



**Fig. 2.3** - Interactions between CAD, CAM, CAE modules

At the end of this stage based on the interaction of the 3 modules are defined: the operation plans, the types of tools, as well as the characteristics of the working points of the manufacturing architecture necessary to make the product.

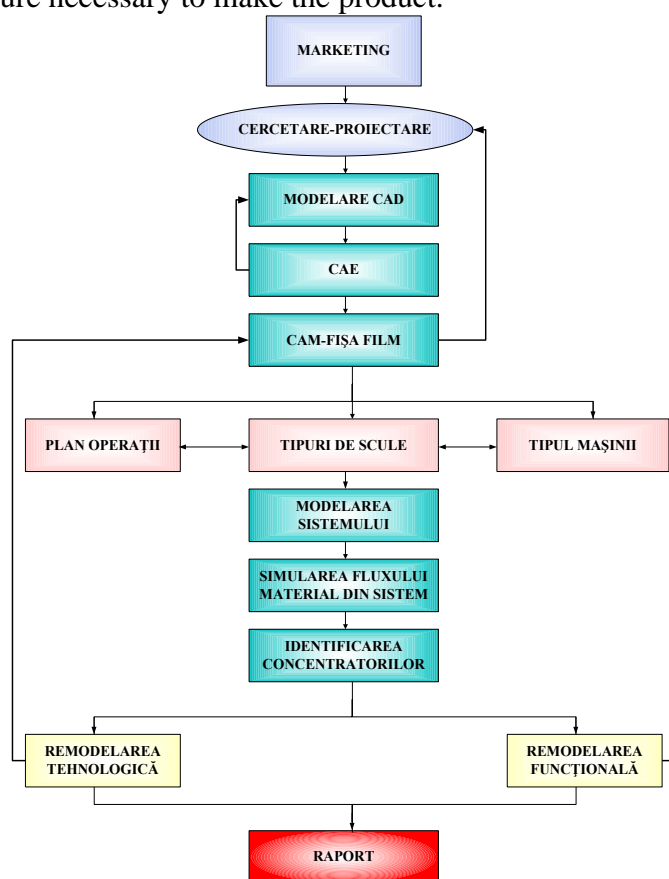


**Fig. 2.4** - Methodology for making a new product

In the Fig. 2.4 presents schematically the methodology of making a new product based on the chronological sequence of these modules from the market research necessary to integrate the customer's requirements in the product sheet until the start of manufacturing. They include the methodology used in the thesis, focused on the interaction of Fig. 2.4.

The sequence of the immediately following modules is the object of material flow management (MFM) and represents a direction for further research in the thesis.

### Chapter 3. Innovative elements assumed through the objectives and structure of the thesis starting from existing methods and solutions

Using a car to cover short distances in urban areas leads to a massive urban agglomeration, most often generated by the fact that on average, the car is occupied by one person, maximum two. According to a study carried out by Tom Tom company for Bucharest, the degree of congestion can be observed depending on the days of the week and hours. [12].

This study highlights the degree of traffic congestion, from which it can be concluded that the busiest hours of the day are between 7 - 9 am and 15-19 pm.

	Sun	Mon	Tue	Wed	Thu	Fri	Sat
12:00 AM	6%	2%	2%	3%	3%	5%	6%
	4%	0%	1%	1%	2%	2%	4%
02:00 AM	3%	0%	1%	1%	1%	1%	3%
	2%	0%	0%	0%	0%	0%	2%
04:00 AM	1%	0%	0%	0%	0%	0%	1%
	0%	1%	0%	0%	0%	0%	1%
06:00 AM	0%	23%	23%	22%	21%	19%	3%
	0%	73%	72%	72%	69%	61%	7%
08:00 AM	1%	92%	93%	93%	88%	77%	13%
	6%	73%	76%	76%	72%	63%	21%
10:00 AM	12%	52%	57%	59%	57%	54%	29%
	17%	50%	55%	57%	58%	58%	36%
12:00 PM	22%	52%	57%	59%	62%	63%	40%
	23%	51%	56%	59%	63%	66%	38%
02:00 PM	21%	49%	54%	56%	61%	74%	33%
	19%	51%	55%	56%	62%	75%	26%
04:00 PM	19%	65%	71%	72%	77%	80%	22%
	22%	89%	95%	96%	100%	89%	21%
06:00 PM	23%	87%	92%	93%	96%	83%	22%
	22%	49%	54%	55%	59%	52%	20%
08:00 PM	20%	25%	28%	29%	32%	30%	18%
	14%	16%	17%	18%	19%	20%	15%
10:00 PM	9%	10%	10%	12%	13%	14%	12%
	5%	5%	5%	6%	7%	9%	8%

Fig.3.1 - The degree of traffic congestion depending on the hours and days of the week [12].

The study conducted by APH reveals that users of alternative means of travel in urban areas are represented by people aged between 18 and 29 years [13].

The design of cars, in recent years, usually consists of design iterations keeping similar characteristics on several platforms in terms of engine, size, transmission, number of seats, etc. The advent of electric or hybrid cars has been in the same design language trying to integrate among cars with heat engines.

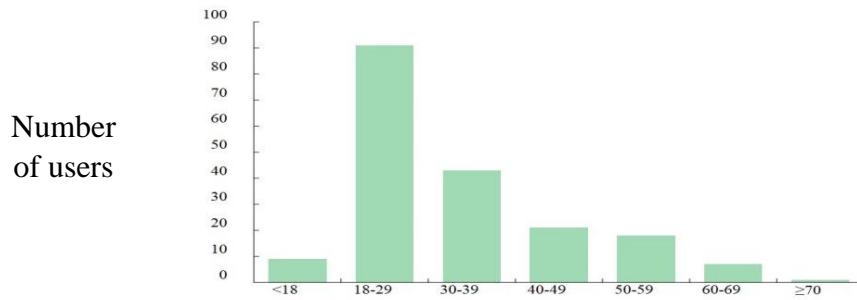


**Fig.3.2** - Age groups traffic study by age groups [13].

Due to the saturation of the market in terms of cars and the inconvenience caused by the exclusive use of public transport, the general requirement has been for small vehicles, preferably electric vehicles, to ensure that the distance from point A to point B is covered, with a high degree of comfort, which can also be used to complete the route that a user can travel with a means of public transport, for example the metro.

Until recently, the general alternatives were represented by different models of bicycles or motorcycles. The freedom of movement offered by the two types of vehicles is desired by every user, but a classic bicycle is difficult to transport and store in cars or public transport, and the motorcycle does not provide a high degree of safety for each category of users.

In fact, the tricycle is suitable for each group of users due to the stability it offers while traveling and the various tilt systems, which have many models of tricycles, make their riding experience comfortable and pleasant.

The idea of smaller and more efficient vehicles is one of the reasons to consider tricycles as a viable alternative in transport design. There are very divided opinions on this proposal. One category is represented by those who see tricycles as a practical solution, due to its mechanical simplicity, low production costs and maneuverability, and another category, claiming to have cornering stability problems.

One of the possible solutions that have been implemented for both human propulsion and electric tricycles is the ability to bend in curves, emulating the principle of 2-wheeled vehicles, which, in addition to a classic vehicle has a stability and a higher degree of comfort.

The design of such a vehicle can be an excellent solution to solve the problem of personal transport, by combining the advantages of safety, stability and comfort of today's cars, with the dynamic handling and compact size of motorcycles, reducing urban congestion.

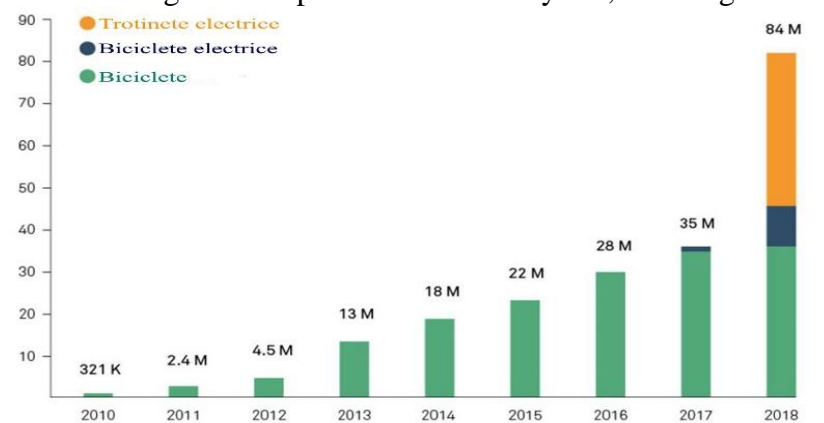


**Fig.3.3** - Increasing the number of electric bicycles, electric scooters - Trips in 2018 [13]

In conclusion, the market is ready for this change from traditional vehicles to small, 3-wheel, electric and folding vehicles.

### 3.1. The objectives of the doctoral thesis

Designing and building a three-wheeled vehicle (tricycle) for personal use, powered by a battery and an electric motor, which has the ability to tilt to increase its stability and give the user a feeling of handling similar to motorcycles solves the problem individual transport.

Objectives:

- 1) Analysis of the technical documentation, in order to understand the physical behavior of this type of vehicle, in addition to the aspects that must be taken into account for its design.
- 2) Studying different projects that have been implemented in order to solve the problem of personal transport and decongestion of urban areas.
- 3) Analysis of similar vehicles on the market in terms of design, ergonomics and user interaction with the product, in order to establish the general benchmarks for the design of this product.
- 4) Generating design solutions, taking into account the different configurations that this type of vehicle can adopt, respecting the road legislation in force.
- 5) The greatest possible use of standardized materials and components to make the product with the lowest possible costs.
- 6) Analysis of the proposed alternative concepts based on the list of requirements imposed on the design, in order to select the best design alternative.
- 7) Making a functional prototype at a scale of 1: 1, in order to visualize the proportions, ergonomics and degree of operation of different mechanisms.
- 8) Testing the vehicle, using computational tools, to determine the behavior of the vehicle in a virtual environment.
- 9) Exposing the concept in the public space and testing it.
- 10) Registration of the innovative solution at OSIM in order to patent it.
- 11) Product optimization in order to find potential manufacturers for the production and marketing of the tricycle.

### 3.2. The structure of the doctoral thesis and the topics addressed in each chapter

The elaborated doctoral thesis is structured on 8 chapters, contains 181 pages, 204 figures and graphs, 19 tables, 32 mathematical relations, 146 bibliographical references, of which 7 belong to the author.

Chapter 1, entitled “**Life cycle instrumentation for the design and construction of a new product**”, presents general aspects regarding the need for this product, the requirements it must meet, concept and design.

After the design stage, aspects related to the functionality of the product, its packaging, maintenance, withdrawal or further development of the concept can be established.

In Chapter 2, entitled “A brief study of the method”, presents schematically the methodology of making a new product based on the chronological sequence of these modules from the market research necessary to integrate the customer's requirements in the product sheet until the start of manufacturing. They include the methodology used in the thesis.

In Chapter 3, entitled “**Innovative elements assumed through objectives and structure thesis starting from existing methods and solutions**”, general aspects are presented regarding the state of the current urban agglomerations, of the types of electric vehicles found on the market an analysis of the current state of the world on the achievements in the field of electric vehicles is made, as well as a market study on development trends for

new ecological transport methods in the urban environment and possible solutions to decongest traffic in these areas.

In Chapter 4, entitled “**Manufacturing methods and technologies for metal structures**“, technological methods and available materials for making such a vehicle are presented, as well as the standardized components that make up the final product. The ergonomic study necessary for the development of such a product is also presented.

In Chapter 5, entitled "**Presentation of the innovative method of design and implementation of a new product for an electric vehicle case study** ", it presents the methods and stages of theoretical and practical research of a three-wheeled electric vehicle as well as the original proposed variants and it presents a theoretical analysis of the previously proposed electric vehicle variants which determines the optimal design variant of an electric tricycle.

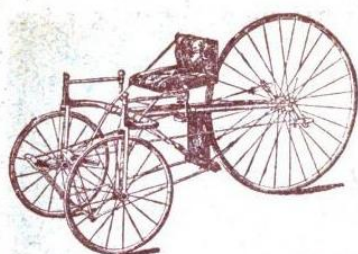
Chapter 6, entitled "**Experimental determination for the validation of the innovative five-stage design algorithm**", presents the stages of experimental analysis which determined the optimization parameters of the components of which the electric tricycle frame is composed.

Chapter 7, entitled "**Algorithms for optimization by parametric resizing of the metal structure**", presents the results of measurements performed in experimental research conducted in Chapter 4. Based on the results were determined the average values of qualitative working and operating indices, establishing the optimal working regime of the tricycle according to the user's mass, the speed of the tricycle and the surface on which it moves.

Chapter 8, entitled "**Conclusions**", presents the conclusions resulting from theoretical and experimental research conducted with the tricycle, as well as the author's personal contributions to optimizing the kinematic, dynamic and energy regime of the electric tricycle.

### 3.3. Performance and limitations of current technical solutions. Characteristics of the electric vehicle case study

The concept of a three-wheeled vehicle was developed after the seventeenth century for the transport of people and products. The first approaches focused on the position of the drive wheel, such as Delta and Tadpole models and manual or electric gear systems. In the case of Delta tricycles, the drive is often on one of the rear wheels, although in some cases both wheels are driven by a differential.[14] [15]. Tadpoles generally use the rear-wheel drive of a bicycle and for this reason are usually lighter, cheaper and easier to replace and repair.[15] [16]. This paper addresses the development of a tricycle equipped with a Delta and Tadpole type gear system.



A



B

Fig. 3.4 - The Tadpole Tricycle [16], B Delta tricycle [14]

#### Non-tilting tricycles

The general concept of a tricycle that does not have a special tilt system, can have a curved behavior similar to a 4-wheel vehicle, this is due to the fact that the center of gravity is placed as close as possible to the common axis of the two side wheels. . For this system to

work, the ratio between the width and height of the tricycle must be taken into account, as it is directly proportional to the resistance it can generate to overturning.

As Robert Riley explains in his paper "Three-Wheel Cars", a simple way to model the safety margin of conventional tricycles in relation to overturning is to build a cone using the height of the center of gravity and the maximum lateral forces, which are determined by the coefficient of friction between the tires and the tread. If the resulting maximum rotational force is projected towards the pavement, the base of the cone is formed, taking into account that the force is equivalent to 1G, the vehicle will result in an angle of  $45^\circ$  between the base plane and the cone generator. If the base of the cone is outside the actual area of the tricycle, it will slip; on the contrary, if the circle falls within the actual area, the vehicle will slip rather than follow the normal trajectory [17].

In order to be able to identify the optimal variant of the tricycle shape, we analyzed both the variant of a tricycle with a front wheel and two rear wheels that will be called 1F2S, and the variant with two front wheels and a rear wheel that will be called 2F1S.

Following a preliminary analysis, the difference in center of gravity can be seen, which in the 1F2S variant is closer to the rear axle. [18], while in the 2F1S variant the center of gravity is closer to the two front wheels.

In the case of the classic tricycle without tilt systems, the manufacturers have taken into account the ratio between its width and height, to reduce the risk of overturning when cornering, but using a special system to tilt the tricycle, these aspects are no longer a limitation.

Although motorcycles do not have side wheels, they can counteract cornering. This is due to the fact that the user tilts the motorcycle towards the turn, to counteract the centrifugal force and the effect of the pendulum acting on it.

As can be seen in Fig. 3.5, while the angle of inclination of the motorcycle correlates with the resulting vector of the forces that appear in rotation (centrifugal force + weight), the motorcycle will not skid, as long as the traction limit between the tires and the asphalt is not exceeded. It follows that a motorcycle has a different angle of inclination on dry asphalt and wet asphalt.



**Fig. 3.5** - The lateral tilt of a motorcycle to counteract the centrifugal force. [19]  
(green - centrifugal force, blue - gravitational force, yellow - resultant force)

Therefore, the design that has a single front wheel and two rear wheels (1F2S) tends more to oversteer, while the design that has two front wheels and a single rear wheel (2F1S) tends to oversteer more.

Another aspect to be analyzed is the behavior of the two tricycle variants in terms of braking and acceleration. When braking in a curve, the tricycle with the 1F2S variant tends to destabilize slightly compared to the 2F1S variant. The maximum braking force is determined by the limited grip of the three tires, while the acceleration is affected only by the traction wheel which can be one, two or three depending on the model chosen.

Given that the force generated on braking is greater than that generated on acceleration, the 2F1S is considered safer for designing a tricycle with a higher engine capacity that can reach higher speeds.

This system uses a rigid chassis to which the three wheels are attached as if it were a conventional tricycle. This chassis does not have the ability to tilt in curves.

An example of this type of configuration is "Acton M", proposed by the company Acton in 2013, presented in Fig. 3.6.



Tricycle Acton M



The Acton M tricycle making a turn where one of the wheels rises from the ground

**Fig. 3.6 - Tricycle Acton M[20]**

This configuration is less adapted to road vehicles due to the mechanical difficulties generated by the small tilt axis, given that the space allocated to the possibility of tilt is limited (Fig. 3.6). For this type of fixed-chassis tricycle, the tilt means that the axle gauge is larger than desired, which is why this type of vehicle may have overturning characteristics similar to a non-tilting car. Contrary to constraints, benefits can be identified for passenger comfort, as the inclination reduces the lateral forces acting on it.

### **Tilting tricycles**

There are different configurations for tricycles that allow tilting.

V3-wheeled tires that can have the ability to tilt in curves, similar to motorcycles, but for this phenomenon to be possible must take into account other types of physical and geometric phenomena. For example, a vehicle with a wide chassis, at a minimum angle of inclination can touch the ground, which is why the behavior of this type of vehicle, in the curve, would not differ much from that generated by a classic car. [21].

### **Limiting the inclination of a tricycle**

Motorcycles have a limit inclination between 45 ° and 50 ° before the widest complicated part of the motorcycle body to touch the ground. These angles represent a lateral acceleration of rotation between 1 and 1.2 G (see equation 2-1).

Equation 2-1 The relationship between the angle of inclination and the lateral acceleration is counteracted.

$$a_L = \tan(\alpha) \quad \text{3-1}$$

where:  $a_L$  is the lateral acceleration;

$\alpha$  is the angle of inclination of the motorcycle.

Motorcycles have a single traction wheel, as a result, there is a single angle of inclination for certain conditions. On the other hand, tricycles that tilt freely like a motorcycle have a wider range of possible tilt angles before they lose control and overturn.

Tilts that allow tilting have gone through all stages of construction by ticking all wheel configurations, from the tricycle that does not allow the tilt of any wheel to the tricycle that allows the tilt of the three wheels.

### **Classification of tricycles according to the inclination configuration**

Another obstacle that represents an obstacle for engineers and designers alike was the adaptation of different propulsion devices so that they are effectively correlated with devices that facilitate the inclination of the tricycle, an obstacle that was removed as a result of mounting the electric motor in the wheel.

In the case of the 1F2S tricycle model the engine is located in the front wheel, being at the same time responsible for turning, and in the case of the 2F1S tricycle model the engine is located in the rear wheel, the front wheels being responsible for turning, the latter model having the possibility of using another propulsion system in order to be able to build a hybrid gear system.

### **By number of wheels:**

One-wheeled tricycle



This vehicle has a tilt system that allows the front axle to tilt individually relative to the rear axle. An example is QugoEroare! Fără sursă de referință., which has a configuration (1F2S) and a tilting system composed of a flexible mechanism which allows the user to tilt in corners like a motorcycle. It is easy to use offering freedom and flexibility, the balance not being mechanically adjusted, having a virtual axis of rotation that moves according to the angle of inclination [22].

### **Tricycle 1F2S and 2F1S with three tilting wheels**

Tricycles that have the possibility of tilting for the three wheels are considered to be the only ones with a sufficiently stable configuration, for very narrow vehicles, with either a 1F2S or 2F1S wheel configuration. This type of configuration can be inefficient for wide vehicles, as the relative movement between the side wheels becomes excessive for large tilt angles.

Both types of tricycles in this category have certain inclination characteristics determined by the distance between the side wheels. [2. 3].

If the distance between the side wheels becomes longer, the maximum angle of inclination decreases for maximum wheel displacement, which generates an inclination limit. If this inclination limit is below the requirement for coordinated curves, then the vehicle is not adapted to be used with a complete natural inclination and a certain type of active control generated by the implementation of a special system is required.

### **The tilt mechanism**

The tricycle can have a free tilt system like a regular motorcycle, but also an assisted system, which is responsible for tilting the vehicle.

Active tilt systems work with hydraulic or electromechanical actuators, which are operated under the signals of an electronic control unit (ECU). Normally, the UCE processes the signals from the sensors that monitor the lateral acceleration, vehicle tilt, steering angle and other relevant factors, and then sends the information to the respective tilt actuators. Another advantage of the active control system is that the user does not have to balance the vehicle as in the case of the motorcycle. With the control system active, the vehicle is driven in the same way as a regular vehicle, as the system handles the rest of the operations.[17] [24].

On the other hand, the unassisted tilt system is much simpler, because as in the case of a motorcycle, the user determines, through his interaction with the vehicle and the terrain conditions, the most suitable angle to take a turn. If it is desired to simply satisfy a need for comfortable transport from point A to point B, an assisted tilting system is ideal. On the other hand, if you want to satisfy a desire for more sporty driving, in which there is a more direct interaction with the vehicle and the road, an unassisted tilt system would be more appropriate.

When maneuvering a motorcycle or bicycle in a turn, in the event of a correction of a much too aggressive tilt, the user must lean slightly to the right if a left turn is desired. This phenomenon is called counter-direction and is used naturally, thus obtaining the required cornering speed even in extreme conditions.

Tony Foale, author of "Motorcycle Chassis Design," explains the behavior of an all-wheel-drive vehicle with respect to a virtual motorcycle between the two side wheels (see Fig. 3.7). In a balanced turn, the resulting force remains aligned with the wheel of the virtual motorcycle; but in curves taken above the tilt limit, the resulting force is projected out of the virtual wheel [25].

When calculating the tilting limit of a tricycle with an inclination limit, the displacement of the center of gravity due to the angle of inclination (the center of gravity of the vehicle moves inwards as the vehicle tilts on the curve), the limiting force must be taken into account. friction between the wheels and the asphalt, the relationship between the height of the center of gravity and the slope limit, as well as the wheelbase.

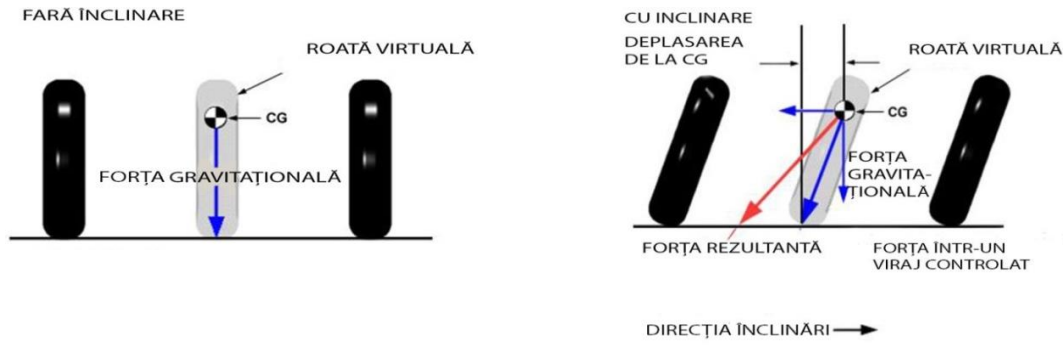


Fig. 3.7 - Virtual wheel method [17]

The segment of the non-tilting frame will behave similarly to a conventional non-tilting tricycle, its main parameters being the distance between the side wheels and the location of the center of gravity.

On the other hand, the tilting frame is analyzed as a virtual motorcycle whose rear wheel will make contact with the ground at a point determined by the height of the axis of geometric rotation.

An important aspect is to locate the geometric axis of inclination of the back as low as possible. However, in a properly balanced turn, the height of the center of gravity of the tilt segment is of no importance in terms of overturning, but will have an influence on the tilt response and on the longitudinal load transfer under braking and acceleration.

#### Elastic suspension system

Currently, there are several elastic damping systems, designed and used by several companies, with various shapes and solutions depending on the tasks they have to bear and perform, as appropriate.

One such system is the RoSta System, being among the first identified. It was born in the mid-40s, being designed by the Rohr, in the village of Staufen, hence the name of the system widely known today. [26]

It initially used a simple, low-cost solution to support the axles of truck trailers.

Neidhart type suspension [27] for vehicles can be mathematically modeled using a second-order nonlinear ordinary differential equation.

$$J\ddot{\phi} + M_r(\phi, \dot{\phi}) = M(t) \quad 3-2$$

In (2-2),  $J$  is the moment of inertia of the suspension given by the half of the mass  $m$  requesting the suspension, and the distance at which this action is exerted is  $\delta$ [27].

$$\phi(t_0) = \phi_0, \dot{\phi}(t_0) = \dot{\phi}_0 \quad 3-3$$

Initial condition.

$$J = m\delta^2 \quad 3-4$$

$M(t)$  is a moment of excitation applied to the suspension, generated by the contact between the wheels and the running track

The behavior of the system is given by the characteristic moment of resistance  $M_r(\phi, \dot{\phi})$ , the shape of which was chosen taking into account the load-discharge characteristic of the suspension [27].

The nonlinearity of the model is given by the characteristic curve of the suspension, which cannot be satisfactorily modeled with a linear model. The model can be used to improve the road holding quality of the vehicle equipped with such a suspension by specifying a wide range of excitation frequencies that affect the grip and thus the direction of the vehicle, or by adjusting the geometric parameters of the suspension or other vehicle-related elements.[27].

**Table 3-1 - DR-C type rubber suspension unit [28]**

Elements Nominal size X length	Couple MD [Nm] angle $\pm \alpha$						PTO Mk [Nm] angle $\pm$ $\beta$ 10	Radial displacement Loading		Axial displacement Loading	
	50	100	150	two hundred	250	300		$\pm$ Sr [Mm]	Fr [N]	His $\pm$ [Mm]	fa [N]
60 X 150 two hundred	75	170	300	460	700	1010	90		5400		1600
	95	220	385	610	930	1380	25	1.0	7200	1.0	2200

The RoSta system is mainly used for various types of recreational and utility trailers,

RoSta elements have multiple functions, acting as torsion spring and support with anti-vibration pivot. Given that it has an operating angle of +/- 30 degrees, with different dimensions, it can have different varieties in the construction of a mechanism [28].

Advantages and benefits:

- fewer components to mount;
- faster assembly and fewer storage items;
- cost advantage;
- does not require maintenance time;
- high productivity.

The torsion axles offer a suspension system that ensures better and easier handling, which means safety and comfortable operation.

The differences between the lamellar spring system and the torsion-axis system are significant.

The torsion axles resist the movement of the wheels by torsional or torsional forces. Inside, a tube or housing steel bar is connected to a traction arm. The axle housing is mounted directly on the trailer frame, while the wheel is mounted on a hub at the end of the traction arm. As the wheel moves its arm up and down, the arm twists the steel bar. It resists and exerts force against the effect of movement. Rubber pads are often compressed and inserted between the flat sides of the steel bar and the housing, further mitigating unwanted movements.

Traction arms are pivot arms used by torsion shaft systems. Most traction arms allow you to adjust the height so that you can return to normal after exercising your function.

The Flexiride system can also be used as two separate side-mounted units that do not require a connection coupling system [29].

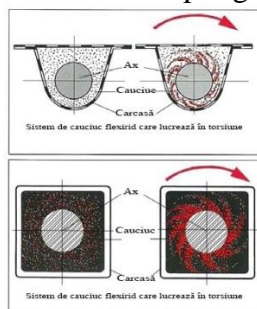


**Fig. 3.8 - Flexiride system with solid rubber**

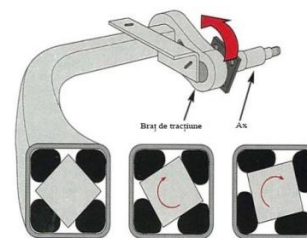


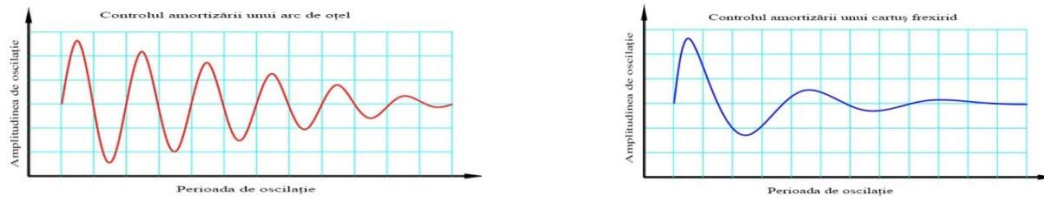
**Fig. 3.9- The system Torflex and RoSta with cylinders rubber**

The Flexiride solid rubber system works by friction rather than compression, ensuring a more angular conformation, a better damping effect and a smoother ride. [29].

systems Torflex and RoSta use square profiles that have 4 rubber cylinders inside that support and react to the movements of another square profile [29].

In the graphs below you can see the difference in shock absorption depending on the suspension system used. In the case of suspension on the spring, the period of oscillation is

longer, regardless of whether only one of the wheels passes over an obstacle. In the case of a suspension in which a torsional axle system is used, the period of oscillation is smoother and shorter, due to the fact that each wheel moves individually. [29].



a) Damping control of a steel spring

b) Damping control of an elastic system

**Fig. 3.10-** The difference in shock absorption depending on the suspension system used [29]

Most torsion systems allow the manufacturer to adjust their damping capacity so that they are neither too rigid nor too weak, a process that uses progressive torsion, taking into account the load that the vehicle bears. [29].

This system can be easily used for various purposes, replacing the coil spring suspension, the lamellar spring or hydraulic spring system.

This chapter has developed the first stage of the design process, which aims to conduct a general study of what already exists regarding this type of vehicle and the demand in the current market.




### 3.4. Limitations of existing products on the market

In this subchapter we analyzed the most relevant models of tricycles made in recent years and prepared a synthetic table with the main technical characteristics of tricycles, which extracted the data necessary to determine the optimal characteristics of these types of vehicles that can be observe in Table 3-2 and Table 3-3.

**Table 3-2 - Market research**

Product features				
	1 Acton M [20]	2 Qugo [22]	3 Yikebike [30]	4 Volta VT3 [31]
Wheel configuration	1F2R	1F2R	1F2R	1F2R
Frame from	aluminum	aluminum	Aluminum / Carbon	Steel
Inclined wheels	0	1	3	0
Maximum passenger weight	300 kg	120 kg	100 kg	130 kg
Full speed	19 km / h	25 km / h	23 km / h	20 km / h
Autonomy	24 km	25 km	20 km	60 km
Battery	Lithium Ion	Lithium Ion	Lithium Ion	Lead acid
Charging time	2h (Fast charge)	2-3 h	1.5 h	6-8 p.m.
	4h (Normal charge)			
Own weight	31 kg	34 kg	15.4 kg	59 kg
Dimensions (L x W x H) mm	970x520x785 (folded)	1150 x 580 x 780 (folded)	660x490x580 (folded)	1210x800x1230
	1020x655x1210	1150 x 580 x 1350	1040x640x825	
Actuating power	500 W	600 W	200 W	350/800 W
Wheel size	24 "	24 "	20 "	14 "
	3"	3"	8 "	2.5 "
Price	£ 1000	€ 2,575.00	\$ 4,995- \$ 7,495	4200 Lei

**Table 3-3 - Market research**

Product features			
	5 Kangaroo [32]	6 Tritown [33]	7 S3trStreeter [34]
Wheel configuration	2F1R	2F1R	1F2R
Frame from	aluminum	aluminum	Steel
Inclined wheels	3	3	3
Maximum passenger weight	-	-	120kg
Full speed	10 km / h	25 km / h	28 km / h
Autonomy		32 km	30 km
Battery	Lithium Ion	Lithium Ion	Lead acid
Charging time		3 h	
Own weight	64 kg	40 kg	38.8 kg
Dimensions (L x W x H) mm	750x550x440	1,140 x 620 x 1,140	1050 x 650 x 1350
Actuating power	-	500 W	400 W
Wheel size	12 " 10 "	14 "	20 " 8 "
Price			

Following the analysis of the main characteristics of the most relevant electric tricycles on the market, the following aspects can be observed.[35]:

- Tricycles predominate in the configuration with one front wheel and two rear wheels, usually tilting with maximum dimensions of up to 24 inches, with an own weight between 15 -64 kg. They usually have the possibility of folding and can reach speeds of up to 25 Km / h and are equipped with a single wheeled motor with a power of 200-800 W.
- The predominant material for their realization is aluminum alloy with small exceptions in which composite materials are used. The use of Lithium-Ion batteries predominates, due to their low weight.

## **Chapter 4. Manufacturing methods and technologies for metal structures used in the construction of the new product**

After researching several models of electric vehicles, such as Asian, European and American, we identified some common points in terms of manufacturing methods and technologies.

Each manufacturer seeks to bring to market an electric vehicle for individual transport with the smallest possible size, with a weight that is easy to handle for each type of user, with a design that is as minimalist as possible, but which, at the same time, is and attractive.

Taking into account the fact that any additional equipment will be reflected in the final costs of the vehicle, we try to optimize the consumption of raw materials necessary for its manufacture.

The basic materials used for the frame are generally aluminum but other light but durable alloys.

### **Metal structure of the frame**

Most manufacturers seek to create a frame that is as flexible as possible, but at the same time stable, made of lightweight materials to facilitate the transport of the entire vehicle without much effort.

Both large manufacturers and small entrepreneurs use lightweight materials to make the frame of electric vehicles. The main goal is to reduce the weight of the whole vehicle, but at the same time to optimize the energy consumption of the batteries. With its low weight, the energy consumed during travel is not wasted just to propel the vehicle.

Although the preferred material for making the frame was, for a long time, steel, newer vehicles with aluminum, carbon, titanium or magnesium alloy frames also appeared on the market.

### **Rectangular pipe profile**

Another variant regarding the architecture of the frame consists in its realization from metal profiles from rectangular or round pipe.

The use of rectangular pipe profiles was chosen due to the adopted suspension system. It involves a series of couplings whose section is square, which involve low manufacturing costs, the damping system being adapted to the standardized size of these semi-finished products. Due to the lower resistance of a rectangular profile to a round profile, the entire subassembly of the frame was oversized.

### **Typical components in the manufacture of electric tricycles**

#### **tires**

The choice of tires must take into account the inclination limit of the vehicle so as to be able to compensate for the remaining centrifugal force which must be controlled by the tires like conventional cars. [36]. If this type of vehicle is to be widely developed, it is necessary to use a type of tire that combines the properties of conventional car tires and motorcycle tires in order to ensure optimum stability in both running and cornering.

On the other hand, the profile and dimensions of the wheels should also be revised according to the dimensions and model of the proposed tricycle. This is because motorcycle wheel profiles are not designed to withstand side loads as large as car wheels.

With regard to the service life of the tires, it must be borne in mind that the inclination increases the wheelbase and therefore introduces lateral tire wear as the vehicle tilts in curves and heads out of the corner. [25].

Another example of an airless tire is NEXO.



**Fig. 4.1** - NEXO airless tire. [37]



**Fig. 4.2** - Exploded view of the e-bike engine [38].

They are easy to mount and last 7-8000 km. In addition, they are made entirely of the same material, which makes them easy to recycle.

### **Engines**

The wheels of electric vehicles, as a rule, also include the motor that drives the entire system, depending on the design of the vehicle.

For electric tricycles, the front wheel is slightly larger than the two on the back and has an electric motor inside that can develop a power between 250 - 500 W.

Hub engines are the first of their kind to be approved for bicycles. Instead of an engine integrated into the bike, completing the chains and speeds that the user uses, the hub motors are completely separate.

They have been adopted on other electric vehicles not only on bicycles. The hub motor is usually positioned in the center of the wheel, thus connecting the tire, rim and axle spokes. The spokes are light and flexible and can absorb some of the shock while walking.

For scooters and electric motorcycles the engine can generate power up to 5000 W.

In the present situation, the drive wheel has a motor that develops a power of 250 W.

### **Batteries**

The most popular types of batteries are lithium-ion or polymer batterieslithium polymer due to the fact that they are very light and do not add unnecessary weight to vehicles.

In most cases, the batteries are embedded in special capsules, attached to the frame of electric vehicles, to be better insulated from the weather, but also to be protected in case of an accident. Many manufacturers choose to buy them from various specialized suppliers. , but there has been a trend lately in which electric vehicle manufacturers also manufacture their own batteries (eg Gogoro - GoStation).

The development of their own batteries, as well as their charging stations, is at the same time a way to control how they are collected and recycled. [39].

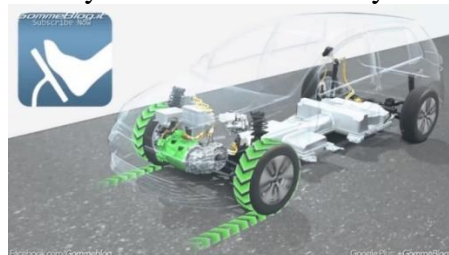


**Fig. 4.3** - Energy regeneration systems [40]

Regeneration systems for kinetic energy lost during braking are mechanical-electrical systems that allow the recovery of energy lost when the vehicle starts to brake. The most widely used form of energy recovery is electric motors, which are used as electric generators together with battery systems.

Batteries used in energy regeneration systems must be resistant to large number of successive charges, as well as have large electrical storage and charging properties (batteries made of Li-ion technology are preferred).

Electric regenerative braking is a process in three stages: the stage of recovering kinetic energy by generating electricity, the stage of storing it in batteries and the stage of using energy by transforming it back into kinetic energy. In all stages there are energy losses, the transformations being made with a certain efficiency [41].

### Ergonomics

For optimal and efficient use of vehicles it is essential that their dimensions comply with a series of anthropometric measures. [42].

Free Rider, a company specializing in cycling equipment, conducted a study focusing on the position of a cyclist using for example and testing various models of handlebars, sleeves and pedals, but correlating with the position that the cyclist misunderstands no matter how good they are ergonomically made components[43].

Thus, the following can be identified as "key" points:

- a) Position of the hands: wrist, palm rest, elbow position;
- b) Position of the feet: center of gravity of the soles, position adopted for pedaling;
- c) Position of the back and pelvis: the muscular tension that predominates in a certain area, center of balance on different types of road.

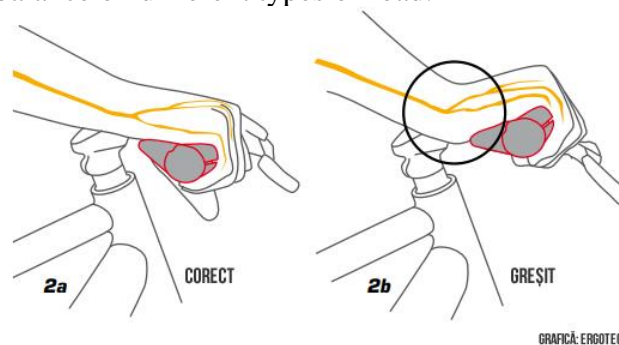


Fig. 4.4 - The positionHand [43]

- a) Position of hands:

It is very important to ensure a correct posture of the user whether we are talking about the classic bike or an electric vehicle.

An incorrect position can cause shoulder, head or neck pain. Equally important is the positioning of the brake levers so that they allow braking effectively without forcing the user's wrists. Depending on the position on the tricycle, the brake levers must follow the arms, thus creating a straight line and releasing the wrists from stress.

As a rule, the handlebars should be as wide as the shoulders, but in the case of a curved handlebar, the positioning of the hands is closer, so a wider curved handlebar can be chosen than in the case of a straight one.

The positioning of the hand determines the positioning of the elbow, and it further has an effect on the shoulders that determines the angle of the back.

The study carried out by Free Rider identified the following solutions for positioning the handlebar on height for bicycles. [43].



## Chapter 5. Presentation of the innovative method of design and production of a new product for an electric vehicle case study

### 5.1. The new product design method

The stages of any design process can be framed in a type of Cartesian plane, in which one axis corresponds to the degree of abstraction, while the other axis refers to the degree of generality. The first step in the design is the abstract generation of the general work plan, which usually starts with the development stage of the constructive sketches of the concept, but in a very generalized way. In this stage the first concrete approximations of what was found in the stage of the abstracted plan are made.

**Planning:**At this stage of the design process, a study of trends, market analysis, research results, patent status and environmental conservation, among others, is performed. This stage is framed in the real plan, based on a study of general ideas, which will serve as a starting point for the particular design.

**Conception:**This step begins with clarifying the problem using as a tool the development of a list of requirements to be met by the device to be designed. It is advisable to classify the system into small "subsystems" in order to continue to identify the best solution for each individual.

**design:**This step is based on the data provided by the design process and aims to be able to give a real shape to the device that is designed. At this stage, we are working again on the real plan, but already having an established design, following the further development.

Following the design stages mentioned above, two general concept variants were developed in the paper, each concept variant proposing a series of iterations of frames aiming at their optimization in terms of shape, weight and ergonomics.

### 5.2. Presentation of the evolutionary design algorithm in five stages for the new product



Fig. 5.1 - Tricycle variants

#### 5.2.1. Stage I

The design and execution stage in this variant was divided into components that were analyzed and developed individually.

The design process aimed at product simplicity, low manufacturing costs and the efficient use of standardized elements.

Due to the lack of a similar product in the university to be studied, the experiments were performed on the product proposed and built by the author, which has the ability to move in a straight line, as well as to bend as stably as possible in corners.

The maximum speed of the vehicle was determined by the power of the electric motor taking into account the weight of the user.

During cornering, the vector resulting from the sum of the weight and the centrifugal force must be aligned with the chassis so that the side loads become only vertical loads.

The weight of the vehicle must be as low as possible to facilitate maneuverability, with as little energy consumption as possible. It is desirable that the weight of the frame be up to 40 kg.

The stability of this curved tricycle must be greater than the stability of a rigid tricycle of similar dimensions. This point is very important when evaluating the quality of the design, because one of the objectives of this project is to develop a three-wheeled vehicle, which has the same cornering stability as a motorcycle, when tilted.

This stage of the design process began with the creation of scale sketches. In view of the proposed objective, the 3D model was developed to determine the proportions of the vehicle, the position of the occupant and the operation of the various mechanisms.

The first solution of this variant consisted of a larger drive wheel on the front and two smaller wheels on the rear. Analyzing the field of use for which this tricycle was designed, the difference in size between the rear and drive wheels makes it difficult to travel on rough terrain and maneuver it in a folded shape.

For the second solution, wheels with the same size were used, thus solving the problem initially encountered regarding passing over obstacles and maneuvering it easily in the folded position, without lifting it from the ground when climbing a curb or steps.

The main components required for the construction of the experimental model (fork arms, battery, motor, wheels and others) were reused from an electric scooter according to its own design (Fig.5.2).

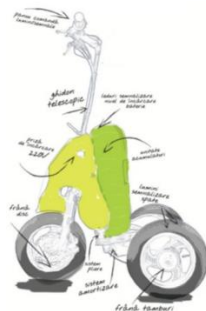


Fig.5.2 - Concept design[44]

After finalizing the sketches, we proceeded to the CAD modeling to finalize the execution project for the tricycle in the 2 folded and normal hypostases with and without applied load.

Based on the modeling in the Solid Works program, the final dimensions of each of the components that make up the tricycle were established:



Fig. 5.3 - Tricycle modeling

### Making the model

A scale model (mock-up) is generally a physical representation of an object, which maintains correct relationships between all important aspects of the model, although the

values of the original properties must not be preserved. This allows a model to demonstrate a behavior or properties of the original object without examining the original object itself. [45].

Models are used in many fields, including engineering, architecture, military command, etc. Scale models are based on the same principles and must meet the same general requirements in order to be functional. The detail requirements are different, depending on the needs of the modeler.

In order for a scale model to accurately represent a prototype, all dimensionless quantities must be equal to the scale model during the observation period and the prototype itself.

For this tricycle, a 1: 1 scale model was built to optimize the proportions and ergonomically verify the concept in order to make the prototype.



Fig. 5.4 - The final shape of the tricycle model

### Realization of the steering system of the prototype

Most tricycles on the market have a steering system in the form of a handlebar that allows the handling of the front wheel. All these mechanisms have the main function of making the center of rotation of the three wheels coincide at the same point, as can be seen in Fig. 5.5.

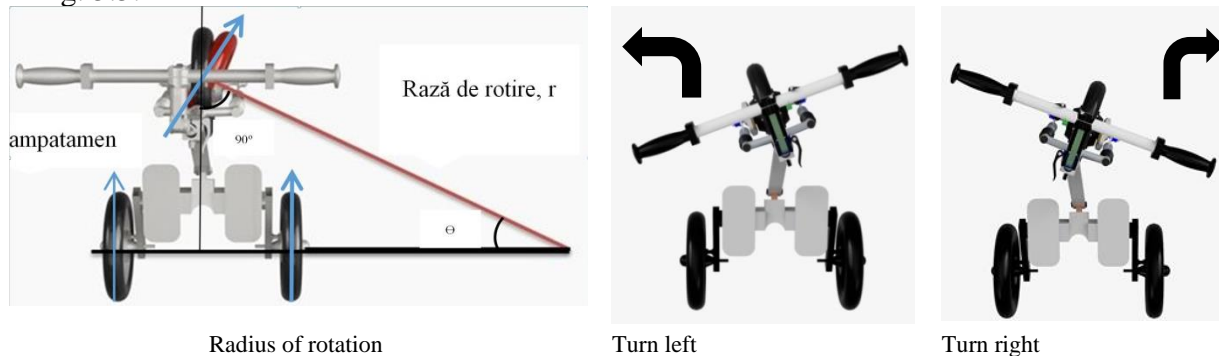


Fig. 5.5 - Steering system

Starting from the fact that a steering system will be used, it must be determined which dimensions of each rod make up the mechanism so that the centers of rotation of the three wheels are approximately the same.

### Realization of the damping and tilting system of the prototype by using the elastic system

As mentioned above in the list of requirements, the tricycle will have an independent suspension system on the rear or front wheels, so that a less complex tilting system can be chosen.

Another factor that has been considered for this tilt mechanism to be implemented is the shape that the arms that connect the chassis wheels will have and how they will be assembled on the chassis so that they can tilt. in relation to it.

As shown in Fig. 5.6, the shape of the arms of the tilt system is designed to absorb frontal forces (on impact or sudden braking).

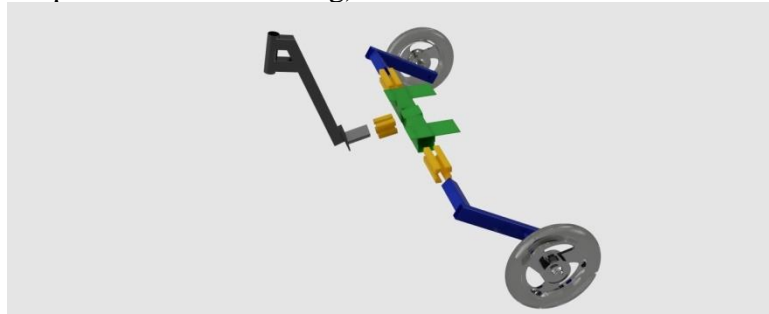


**Fig. 5.6** - Sdamping systemetand inclination

Regarding the way in which the arms will be connected to the chassis, a viable solution would be to use cylindrical elastomers that slide on the profiles that make up the chassis. In theFig. 5.6 you can see how these arms are connected to the chassis.

As the main problem with the stability of the vehicle was the difficulty of resuming its vertical position when it came out of a turn, it was decided on an elastic system, which would have the ability to keep the vehicle upright.

As mentioned above, the tricycle tilting system is an elastic mechanism consisting of a square measuring 60 x 60 mm and a square of 40 x 40 mm rotated at an angle of 45 degrees to the first square and positioned concentric. Four rubber cylinders were pressed in each corner of the original square.

In the Fig. 5.7the principle of operation of this system can be observed, which, when a torque is applied to the inclination of the tricycle (1), a traction force (2) is generated on the opposite side of the inclination. This force of the elastic system generates another torque (3), which tries to keep the tricycle in its vertical position and the two rear wheels maintain the same orientation towards the chassis, ie they will always be parallel to the chassis. With this device it was possible to achieve better stability, because the force required to return the vehicle to its upright position is less and can be counteracted by the weight of the driver's body.

In the Fig. 5.7 the deformation of this system can be seen when the vehicle is tilted to one side.

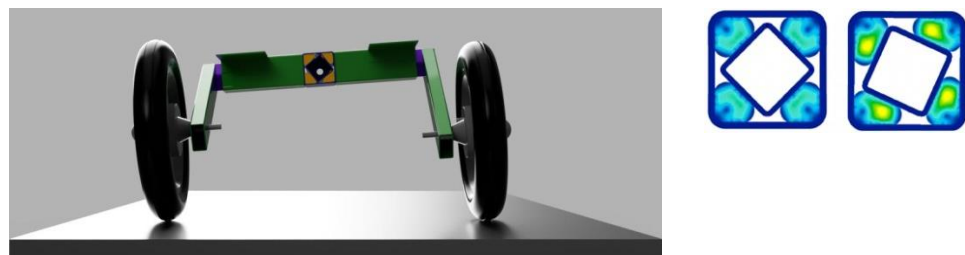


**Fig. 5.7** - Deformation of the elastic system on inclination

### **Considerations on tricycle manufacturing technology.**

Considering the objective of the work to reduce the mass of the tricycle, in this stage of realization of the prototype were taken into account materials and manufacturing technologies that allow the implementation of the prototype in series production, as it resulted from design studies, ergonomics and resistance.

In the context of mass production of the tricycle, each component was designed taking into account the usual technologies found in a specialized company.

In the assembly stage of the finished product, the use of existing technologies and usual fasteners was considered.

The following describes briefly the manufacturing processes and technologies envisaged for each component of the tricycle.

### Tricycle chassis

The chassis is the component that supports all the other parts of the tricycle. The following steps were taken to manufacture it:

1. Choice of rectangular pipe material obtained by cold deformation (steel EN 10219);
2. Choosing the type of semi-finished profile of the dimensions - extruded, rectangular and round bar with section dimensions of 40 x 20 x 2 mm, Ø 40 x 2 mm and length 6000 mm.
3. Cut the necessary lengths provided in the execution drawings to the continuous band saw from the purchased semi-finished bar;
4. Adjustment to prepare for welding.
5. After making all the parts, the assembly stage follows, which is done according to the detailed scheme.
6. Place the parts on the welding table with the help of welding pliers and auxiliary devices according to the design of the chassis part and weld with electric arc.
7. Mounting by electric arc welding in a protected environment (MIG-MAG).
8. Check the dimensions and quality of the chassis parts according to the specifications of the execution drawings and it is allowed if it is a good or rejected part.
9. Electrostatic painting of the landmark given the ral color specification.

When assembling, consider every joint provided with rolling bearings, lubrication with special Metabond grease in order to reduce friction

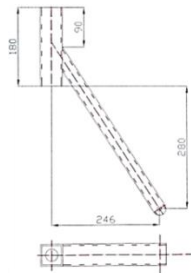
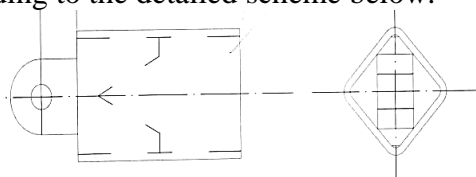


Fig. 5.8 - Tricycle chassis

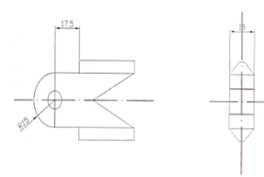
### Tricycle folding system

The folding system is a component used to fold the tricycle. The following steps were taken in its manufacture:

1. Choice of rectangular pipe material obtained by cold deformation (steel EN 10219);
2. Adjustment to prepare for welding.
3. Place the parts on the welding table with the help of welding pliers and auxiliary devices according to the design of the chassis part and weld with electric arc.
4. Mounting by electric arc welding in a protected environment (MIG-MAG).
5. Dimensional and qualitative verification of the Saxon part according to the specifications of the execution drawings and it is allowed if it is a good or rejected part.
6. Electronic field painting of the marker considering the ral color specification.
7. After making all the parts, the assembly step is followed, which is done according to the detailed scheme below.



Tilt system assembly



Central part tilt system

Fig. 5.9 - Tricycle folding system

### **Fork and handlebar assembly of the tricycle**

The fork is the component on which the drive wheel and damping system are mounted.

1. Choice of rectangular pipe material obtained by cold deformation of steel EN 10219.
2. Choosing the types of semi-finished products - rectangular, round pipe, bar, sheet with cross section dimensions of 60 x 60 x 2mm, 40 x 40 x 2 mm, 40 x 20 x 2 mm 40 x 2 mm, Ø 27 x 2 with length of 6 m.
3. Cut the necessary lengths provided in the execution drawings to the continuous band saw from the purchased semi-finished bar.
4. Adjustment to prepare for welding,
5. Place the parts on the welding table with the help of welding pliers and auxiliary devices according to the execution drawing and weld with electric arc
6. The threading is processed by turning on a universal lathe, at the dimensions in the execution drawing, after which the conformity of qualities is checked.
7. After making all the parts, the assembly stage follows, which is done according to the assembly scheme followed by the finishing, painting stage.



**Fig. 5.10** - Fork and handlebar assembly

At the assembly, the joints provided with rolling bearings and the lubrication with special Metabond grease will be taken into account in order to reduce friction and efficiency.

The same will be done at the wheel bearings for the same purposes, to reduce friction.

### **Rear axle of the tricycle**

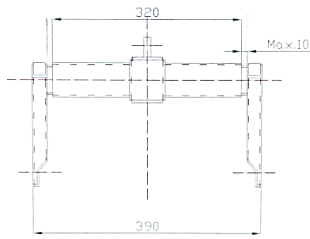
The rear axle is the component on which the drive wheel and damping system are mounted.

1. Rectangular pipe obtained by cold forming, steel EN 10219 is used.
2. The types of semi-finished products are used - rectangular, round pipe, solid bar, sheet with the dimensions of the cross section of 60 x 60 x 2 mm 40 x 40 x 2 mm, 40 x 20 x 2 mm 40 x 2 mm 27 x 2 with a length of 6 m.
3. It is cut from semi-finished bars with lengths necessary to make the components, to the dimensions in the execution drawings.
4. It is cut at the band saw.
5. Place the parts on the welding table with the help of welding pliers and auxiliary devices according to the design of the chassis part and weld with electric arc.
6. The parts are adjusted for welding,
7. The support shaft of the wheel axle is processed by turning on a universal lathe, at the dimensions in the execution drawing, after which the conformity is checked followed by the finishing, painting stage.
8. The damping elements are assembled according to Knott's technology.
9. After making all the parts, the assembly stage follows, which is done according to the assembly scheme.

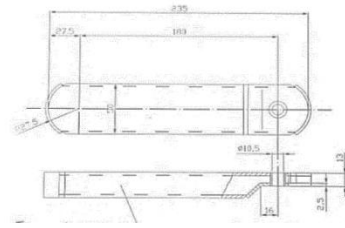
At the assembly, the joints provided with rolling bearings and the lubrication with special Metabond grease will be taken into account in order to reduce friction and efficiency.

The same will be done at the wheel bearings to reduce friction.

## Innovative design and manufacturing method of a new product



Rear deck assembly top view



Rear axle arms left and right in the mirror

**Fig. 5.11** - Rear axle of the tricycle



**Fig. 5.12** - The realization process

**Table5-1** - Technical specifications of the prototype I

Product features	Variant I
Wheel configuration	1R2S
Inclined wheels	3
Frame built of	Steel
Maximum passenger weight	150 kg
Full speed	20 km / h
Autonomy	25 km
Battery	36v 14mA lead acid
Charging time	10 hours
Own weight	42 kg
Dimensions (L x W x H) mm	500x592x910 (Folded)
	910x600x1130
Actuating power	250 W
Wheel size	12 "
Price	5000 lei

### Research on depreciation systems

Following the research presented above the suspension and damping system, it was found that most manufacturers use a tubular profile for the construction of frames, which has an equal strength over its entire surface.

For the construction of the tricycle frame, a rectangular profile was used, which conditioned the appearance of the frame, necessary for the realization of the damping system. Also, the use of a rectangular profile meant low costs and was easier to develop.

To compensate for the fragility given by the rectangular shape, the resistance structure was oversized.

Suspension systems that integrate into the structure of the rubber are found in numerous studies, as this optimizes the control of shocks and vibrations. For example, the study by Zhao can be mentioned [46] where to improve the performance of the seat of a vehicle a new type of suspension was created composed of springs made of rubber-based composite material.

This implementation has led to an attenuation of the low frequency vibrations generated by difficult terrain. For vehicles used for rail transport, pneumatic elastic elements containing rubber are increasingly used as a secondary suspension system. [47].

In aeronautics, the problem of complex installation can be solved by generating new models based on qualitative semantic models. (Analysis of the two-chamber shock absorption system, based on hybrid methodology).

Approaching this analysis requires the development of new models and methods for obtaining information on the shape of the modeled object, which is more important than its structure. In the case of autonomous vehicles, other types of suspension systems have been designed to improve the comfort and maneuverability obtained by dissipating the energy induced by the terrain.

Relevant results from the scientific literature, for example studies by Nielens [48] they focus on mechanical simulations as well as on structures that have better energy absorption.

Studies show that we should be careful before using more suspensions, regardless of the terrain, as handling becomes more difficult. Also, as these systems ensure a good efficiency of the absorption of shocks generated by the irregularities of the terrain and, consequently, obtain a greater comfort, they can generate, an increase of the effort of the passengers, especially for the cyclists.[49].

Unfortunately, studies show that passive vibration absorption systems that use viscoelastic materials due to their nonlinear characteristics with temperature, frequency and mechanical stress lead to nonlinear dynamic properties. Thus, in designing the reliable vibration isolation system from the point of view of the mathematical model and the optimal design, it is necessary to determine the degree of rigidity and absorption of the viscoelastic material influenced by shape and structure.[50].

### A. Theoretical and experimental tests

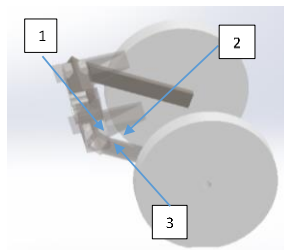


**Fig. 5.13** - 3D model of the individual electric tricycle

a) side view; b) isometric view; c) structure of the system: 1 outer part, 2 rubber and 3 central part.

This chapter analyzes three different vibration damping structures and mechanical vibration damping intended for use in an individual tricycle electric vehicle. Fig. 5.13. The systems are practically used at the level of the support parts of the foot, but they can also be used in the steering system.

The three constructive solutions analyzed are presented structurally and physically in Fig. 5.14 with the following characteristic elements:

The outer part is a rectangular housing with a solid hexagonal central part, see (Fig. 5.14 a).

The outer part is a rectangular housing with a round central part, (Fig. 5.14 b).

The outer part is a rectangular central part with a round housing, (Fig. 5.14 c)

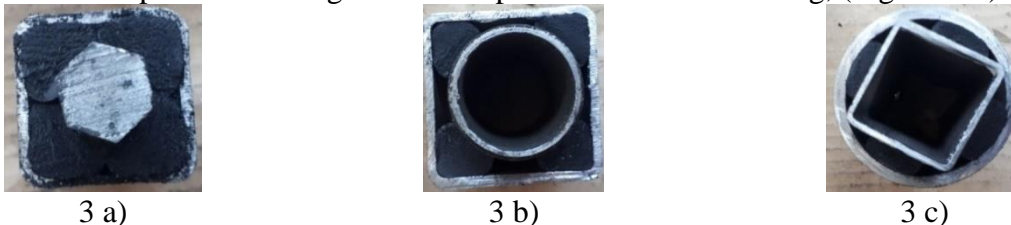


**Fig. 5.14** - Different construction solutions:

a) the outer part is a rectangular housing with a solid hexagonal central part;

b) the outer part is a rectangular housing with the round central part;

c) the outer part is a rectangular central part of a round shell.



The three damping variants were tested for static mechanical loading. In the first stage, a mechanical load was applied, which means applying a torque on the central part. Thus, a test stand was built (Fig. 5.15), on which a set of preliminary tests was performed in which it was found that a mechanical load of 300 Nm is sufficient. For this purpose, a fixing piece was built to allow the installation of each external element of the tested structures. On the central part I fixed a lever with a length of 1 m, and at the free end I attached the manometers with predetermined weights.

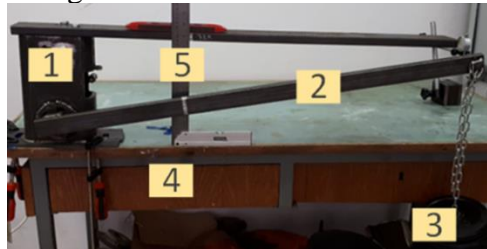


**Fig. 5.15** - Experimental testing for static mechanical load.

1) fixing device for the structure to be tested; 2) bar with a length of 1m; 3) calibrated weights, 4) mass; 5) system for measuring the angle of the bar (considering the horizontal as a reference) and the height.

In the first case, the outer part is rectangular and the central part is the solid hexagon (Fig. 5.14a). Due to the compact structure, neither the outer element nor the central element deforms and thus the rubber will have a large deformation under the considered mechanical load and has a zero elastic characteristic.

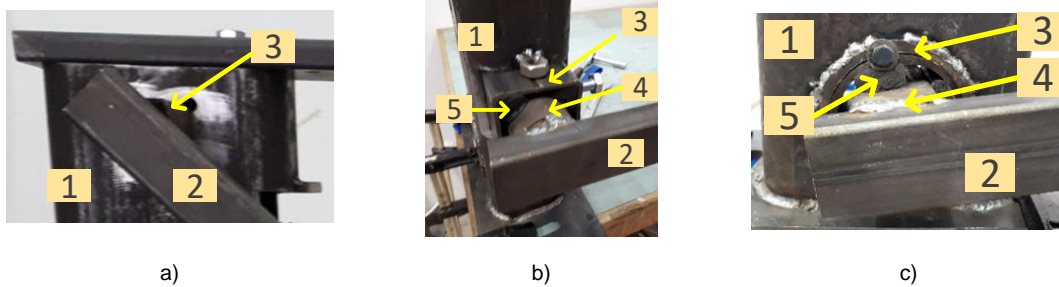


**Fig. 5.16** - Experimental testing for static mechanical load. Fixing part of absorption structures:

a) the outer part is a rectangular housing: 1) the fixing part of the absorption structures, 2) the bar used for applying the moment on the inner part. 3) solid hexagonal central part (hidden); b) the outer part is a rectangular housing: 1) the fixing part of the absorption structures, 2) the bar used for applying the moment on the inner part; 3) outer component of the damping system 4) round central component, 5) rubber; c) (3) the outer part is a round housing (4) the rectangular central component 5), between the components are pressed four rubber cylinders.

In the second case, the elements of the assembly slide between the components on the side of the rubber, thus not obtaining the expected results (in terms of elastic deformation and return to the initial position). In this case, they do not have a deformation, but they slip and the structure does not return to its original position (Fig. 5.17).



**Fig. 5.17** - Experimental testing for static mechanical load.

Permanent movement of the system

1) fixing a part of the absorption structures; 2) the bar used to apply the moment on the inside; 3) the outer part is a rectangular housing; 4) round centerpiece; 5) rubber.

The third configuration of the ensemble performed best in these tests, which is why a dynamic theoretical analysis was made only for this structure. The experimental tests were

confirmed by the results of the simulation of the finite elements. The results are obtained considering the geometry of the structure, the type of material and the type of discretization. After completing the analysis program of the study, there is the possibility to view the results. In the image you can see how the central part is deformed and the elastic element (rubber rod).

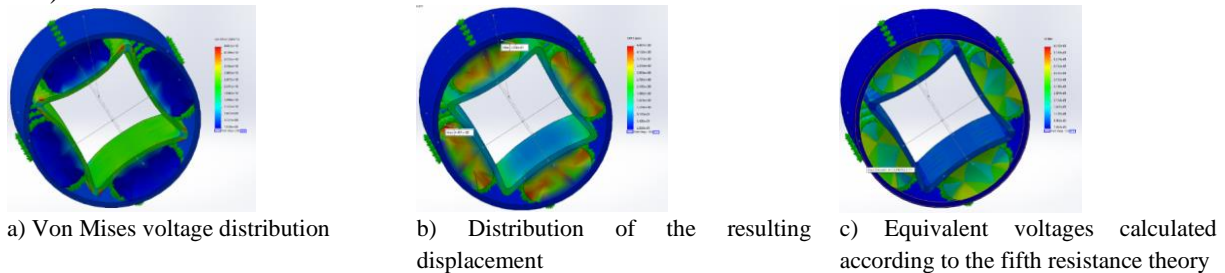


Fig. 5.18 - Finite element simulation results:

## B. Dynamic analysis

Due to the mechanical structure of the vehicle, the shape of the user's weight (the part which can be placed under the supporting part of the legs, as can be seen in Fig. 5.17 and ground level oscillation, three types of mechanical load were identified:

- Compression of rubber elements;
- Bending the outside
- Bending the central part;
- Torsion of the central part.

The first case analyzed is the compression caused by the system itself. The system is much longer than the dimensions of the frame section. The load of the user's body is evenly distributed by the footrest (positions 1 and 2 of Fig. 5.19) which has a central part to the steering system. This harmonic load has been considered because, although the mass is unchanged, when the ground is flat, but has a certain roughness due to the dynamics of the system, the load varies due to its vertical displacement.

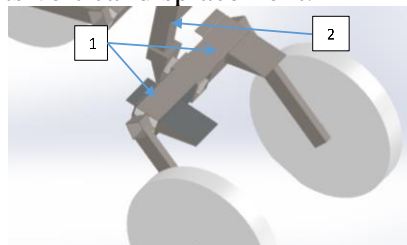


Fig. 5.19 - Position of the absorption system 1 - position of the legs; 2 - the supporting part of the body.

Because the structure has no bearing, it can be said to be a system with linear cubic rigidity. We can write, in this case, from a mathematical point of view the elastic component of the system, in the case of elastic force,  $f_e$ :

$$f_e = k(x + \mu x)^3 \quad 5-1$$

$x$  - vertical deformation of the system

$k$  - rigidity

$\mu$  - the negative nonlinearity coefficient, because it was observed in tests that the system has a descending slope, thus it is represented as a soft characteristic of the elastic component

We consider that when the vehicle is in motion, the force due to the weight of the passenger is harmonic with the magnitude and a small impulse  $\omega$  due to the very low frequency of several Hz which will lead to a harmonic displacement. Since the types of mechanical loading have been separated, it can be considered as a flexible system. The equation of motion can be written in the form, taking into account only the transverse vibration:  $F_0$

$$m\ddot{x} + \frac{gk}{\omega}\dot{x} + k(x + \mu x^3) = F_0 e^{i\omega t} \quad 5-2$$

In equation G is an equivalent structural absorption factor. The study focused only on harmonics and linearity, and the displacement can be described depending on the motion vector:  $\tilde{\alpha}$

$$x = \tilde{\alpha} e^{i\omega t} = (a_R + ia_I) e^{i\omega t} = a e^{i(\omega t + \theta)} \rightarrow x^3 \cong \frac{3}{4} a^2 x \quad 5-3$$

The real component () and the imaginary component () of the system is  $a_R a_I$

$$a_R = \left( 1 + \frac{3}{4} \frac{\omega}{\omega_n} a^2 - \frac{\omega}{\omega_n} \right) \frac{k}{F_0} a^2 = F \sqrt{a^{2 - \left( \frac{gka^2}{F_0} \right)^2}} \quad 5-4$$

$$a_I = g \frac{k}{F_0} a^2 \quad 5-5$$

Considering that the amplitude of the displacement and the phase  $\theta$  angle we can describe the motion vector  $\tilde{\alpha}$

$$a = \sqrt{a_R^2 + a_I^2} \quad 5-6$$

$$\text{tg}(\theta) = \frac{g}{\eta^2 - 1 - \frac{3}{4} \mu a^2} = \frac{g}{\pm \sqrt{\frac{F_0^2}{k^2 a^2} - g^2}} \quad 5-7$$

We rewrite the equations according to the imaginary and the real part and we get

$$\left( \frac{\omega}{\omega_n} \right)^2 = 1 + \frac{3}{4} \mu \frac{F_0}{k} (-a_I) \pm g \sqrt{\frac{F_0}{gk} \frac{1}{(-a_I)} - 1} \quad 5-8$$

$$\left( \frac{\omega}{\omega_n} \right)^2 = 1 + 3\mu \left( \frac{F_0}{2gk} \right)^2 - \frac{3\mu \left( \frac{F_0}{2gk} \right)^2 a_R^2 + \frac{F_0}{k} a_R}{2 \left( \frac{F_0}{2gk} \right)^2 \left[ 1 \pm \sqrt{1 - \left( \frac{2gk}{F_0} \right)^2 a_R^2} \right]} \quad 5-9$$

The equations describe a family of curves above the curve inclined to the low frequencies

$$\omega^2 = \omega_n^2 \left( 1 + \frac{3}{4} \mu a^2 \right) \quad 5-10$$

The pulsation of the system should have a different value from the natural pulsation of the system and in our case we obtained from the finite element model its value of

$$0.07234 \cdot \omega_n = \sqrt{\frac{k}{m}}$$

We can define the stability limit:

$$\left( \frac{\omega}{\omega_n} \right)^2 = 1 + \frac{3}{4} \mu a^2 \pm \sqrt{\frac{9}{16} \mu^2 a^4 - g^2} \quad 5-11$$

$$\eta \left( \frac{\omega}{\omega_n} \right)^2 = 1 + \frac{g}{2} \left( \text{tg}(\theta) + \frac{3}{\text{tg}(\theta)} \right) \quad 5-12$$

The next type of load is torsion for the entire structure. In our case, the equations of motion are:

$$\ddot{\beta} + k_{oi} \beta + k_{1i} \beta^3 + c\beta' = M(t) \quad 5-13$$

where =  $\begin{cases} 1 \text{ pe incarcare} \\ 2 \text{ pe descarcare} \end{cases}$

with the original conditions of:

$$\dot{\beta}(t_0) = 0 \quad 5-14$$

From an experimental point of view, the values between the torque and the torsion angle are obtained and, based on these values, the presented diagram was constructed. Fig. 5.20. It can be seen in Fig. 5.20 that there is a small hysteresis, using only the trend line identified the moment of resistance which can be written as:

$$M(t) = 7.345\beta - 15.387$$

5-15

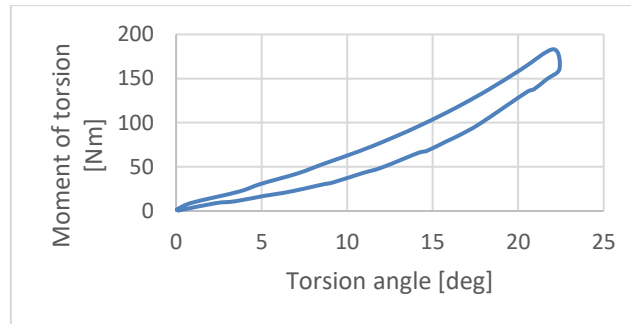


Fig. 5.20 - Torque diagram vs. torsion angle

### Conclusions:

This chapter presents three systems designed to absorb mechanical shock and reduce vibration, which can be used in individual electric vehicles. Experimental tests with static mechanical loads identified the most efficient structure and were validated by finite element analysis. Also, for this structure different modes of simple dynamic stresses have been analyzed which will be integrated in a complex mathematical model that can be used in other similar structures.

In the next step the bending will be analyzed in the simplified case where one wheel does not move and the other moves under the action of the force generated by the terrain deformations when the vehicle is moving, and for the third type of mechanical load, it will be taken into account. consider the effect of the central part [51].

#### 5.2.2. Stage II

Detecting the errors of stage 1, redefining the whole concept and testing and improving the product.

Once the functional model was completed, tests were performed to observe its behavior in order to optimize the product. The following problems were observed:

Changing the fork tilt angle.

It was found that the use of a classic suspension system of spring fork type for the front axle positioned at an inclination of 15 degrees (standard angle used on the fork of a two-wheeled vehicle, electric), during operation changes the geometry of the tricycle over the permissible limit, limiting its use for a certain weight. The temporary solution was to adjust the angle from 15 degrees to 90 degrees, thus obtaining an angle of inclination compatible with the damping system used for the rear axle.

The angle available for short turns was reduced, and the actual testing found the need to improve it to provide a greater degree of maneuverability and safety during use;

The handlebar requires a more ergonomic shape and is easy to fold (the solution identified at this time is by rotation).



Fig. 5.21 - Variant II

Folding type: in the first prototype, folding is done by removing an axle and there is a risk that it will be lost during the process, making it impossible to use the vehicle later.

The small width of the vehicle is a noticeable discomfort over long distances. A wider width would be needed for better walking stability.

Starting from the first prototype, it was wanted to improve the framework and its functions taking into account the problems identified above.

Table 5-2 - Technical specifications of the prototype II

Product features	Variant II
Wheel configuration	1R2S
Inclined wheels	3
Frame built of	Steel
Maximum passenger weight	150 kg
Full speed	20 km / h
Autonomy	25 km
Battery	36v 14mA lead acid
Charging time	10 hours
Weight	42 kg
Dimensions (L x W x H) mm	500x660x700 (Folded)
	880x660x1250
Actuating power	250 W
Wheel size	12 "
Price	5500 lei

### 5.2.3. Stage III

Following the analysis of the functionality of the frame 2, it was concluded that the damping system for the front fork, which was built using the fork arms of the electric scooter, has a limited degree of elasticity. This aspect shows that it does not have very good damping characteristics when crossing an obstacle and does not offer increased comfort to the user, which is why it was decided to replace the front damping system of the electric tricycle.

The optimization of the damping system aims to increase the reliability of the tricycle, the degree of comfort, reduce manufacturing costs and reduce the level of complexity of the final product. The optimization process was achieved by creating a new product, of its own design, made of standardized materials through standard manufacturing processes. Finite element analysis and kinematic study were used to validate the studied frontal damping variants of the tricycle.

A telescopic fork with a helical spring damping element was used for the initial damping system [52]. Following tests, it was concluded that due to the operation of the fork damping system, the geometry of the tricycle frame is adversely affected during operation.

As a first solution, an attempt was made to change the angle of inclination of the frame neck to allow the fork damping system to work correctly. This adaptation led to too much stiffening of the tricycle in the front, which negatively influenced the dynamics of the tricycle (Fig. 5.22).



Fig. 5.22 - Variant II prototype[53]

Taking into account these aspects, the development of a new damping system was taken over, which would take over the damping principle of the elastic type frame (rear axle).[54], eliminating the dynamics problems of a classic telescopic fork.

### 1. Front fork damping study

The study focused on optimizing the structural elements that will make up the new depreciation system. For the new spring-type damping system, two types of structures (geometries) were considered, the first with two fixed arms and a wheel centered between the arms and the second system with two independent arms each with one wheel.

For the finite element analysis, the elastic elements respectively helical spring, rubber and wheels were considered solid bodies, the purpose of the modeling being to validate the metallic structure of the damping system.

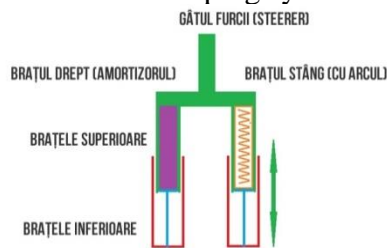


Fig. 5.23 - Helical spring fork [55]

Principle of operation of a telescopic fork: each arm of the fork is composed of two concentric tubes that slide side by side through a system of bushings. In the inner tube is the shock absorption system (spring) and the oscillation damping system (shock absorber). Usually the spring is positioned in the left arm and the damping system in the right arm of the fork [56].



Fig. 5.24 - Fork with elastic damping system

The studies were performed in the Solid Works modeling and simulation program using the “static stress” simulation module.

In order to perform the simulations, the following aspects were taken into account:

- The rear wheels were locked at ground level and the front wheel was left free to slide all over the surface. The variant with all the wheels locked was also tried, the result being static indeterminate. The option of locking the rear wheels and leaving the front axle free was chosen, this constraint having a negative effect on the behavior of the front damping system.
- The mechanical load was distributed at the handlebar and at the foot support point on the frame with a value of 1100 N.
- The voltage state of the frame and the front damping system in the three situations were followed in order to identify the critical areas in which the voltage state exceeds the value allowed for the strength of the material from which the tricycle structure is made.

For the frame variants 1, 2 and 3, the maximum and the lower value of the material from which the elements are constructed were obtained.

Working method:

The structure of the tricycle was fixed on the “xy” plane by the rear wheels with the “roller / slider” type constraint.

The discretization of the structure was done by:

- 264493 elements in 492461 nodes, an element having 5 mm.
- 31446 elements in 453710 nodes, an element having 5 mm.
- 309940 elements in 582256 nodes, an element having 5mm.

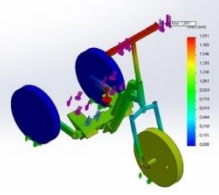
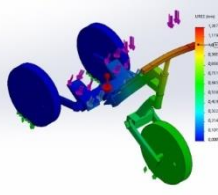
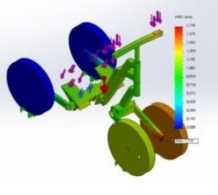
Results

Following the analyzes performed, they can be observed in

Table 5-3 the maximum deformations of the frame, using the 3 different damping variants. In variant 1, using a classic fork-type damping system, following the application of a force of 1100 N, the frame deformed by 1.85 mm, the area with maximum deformation being at the top. By modifying the front damping system, using an elastic damping system, the deformation of the frame was reduced to 1.27 mm. In the damping variant 3 it was wanted to increase the stability of the vehicle, using two wheels on the front, each wheel being provided with an independent viscoelastic damping system. The result of this damping variant can be seen in

Table 5-3 the frame having a maximum deformation of 1.71 mm.

Table 5-3 - Results

Option 1	Variant 2	Variant 3
		
Maximum deformation of 1.857 mm Node: 293374	Maximum deformation of 1,287 mm Node: 8256	Maximum deformation of 1.718 mm Node: 26035

The use of a viscoelastic damping system brings advantages on the stability of the vehicle and offers a better resistance to the frame, eliminating some of the stress states in the structure of the classic fork.

The studies were performed in the SolidWorks simulation and modeling program using the dynamic simulation module. The purpose of these studies is to determine the optimal type of front suspension for this application, taking into account the final costs.

The following aspects were taken into account for the simulation:

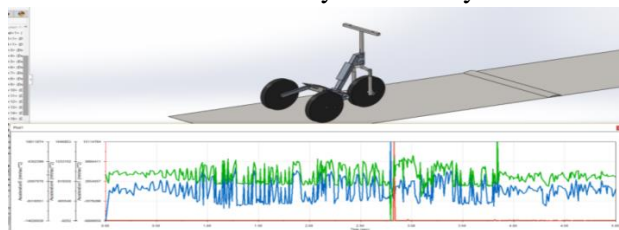
The rear and front wheels were left free to slide over the entire surface, after the surface and contacts were selected in the model.

The mechanical load was distributed at the handlebar and at the support point of the frame legs with a value of 1100 N at 10 km / h, using a 250 W electric motor on the front wheel, as can be seen in the table Table 5-4.

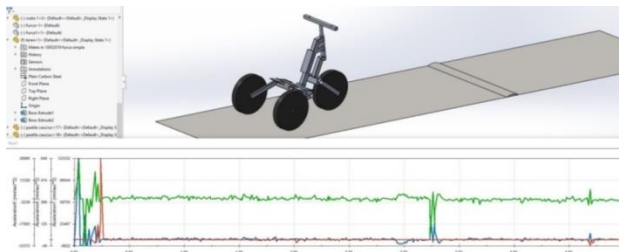
All three iterations were subjected to a short speed limiter obstacle course. The obstacle is 10 cm high at its highest point, with curved entrance and exit surfaces.

**Table 5-4 - Dynamic study**

**Variant 1**



**Variant 2**



**Variant 3**

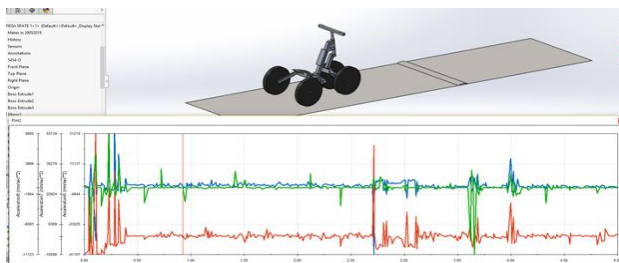
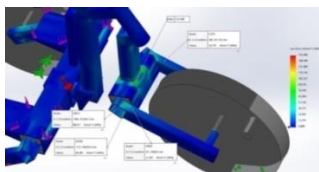
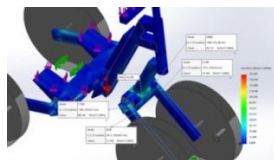


**Fig. 5.25 -** The load used for the kinematic analysis taking into account the user's weight and the damping system

As shown in the results, the optimal type of front suspension is the second iteration using an elastic suspension system with one front wheel. This suspension system has good absorption qualities and also offers a smooth recovery after impact. The second iteration will be used for the further development of the tricycle.



Von Mises (N / mm) 153,460



Von Mises (N / mm) 152,453

**Fig. 5.26 -** Areas where the maximum voltage develops at the fork

The analysis shows that all variants can be used in production given that the strength structure is validated as a development directive.

An obstacle crossing test was also performed, without incorporating a damping system, to determine the maximum values of the forces that will be applied in the finite element structure.

**3d modeling stage III**

**Table 5-5 -** Technical specifications of the prototype III

Product features	Variant III
Model tricycle	1R2S
Inclined wheels	3
Frame built of	Steel



Maximum passenger weight	150 kg
Full speed	20 km / h
Autonomy	25 km
Battery	36v 10mA lithium ion
Charging time	6 hours
Weight	32 kg
Dimensions (L x W x H) mm	530x660x760 (Folded)
	920x660x1250
Actuating power	250 W
Wheel size	12 "
Price	6500 lei

#### 5.2.4. Stage IV

Starting from the analysis of the previously presented frameworks in variant III, the need for a lighter framework was identified. Thus, a new frame was built, made of aluminum profiles.

The profiles used are rectangular, in order to keep production costs low.

#### Aluminum profile

Aluminum has a third of the density of steel, which allows efficient and easy solutions for car components compared to steel, so the weight of the vehicle decreases significantly. Aluminum also absorbs twice as much energy as steel, which means that using aluminum to make a vehicle also increases its safety. Tests to date have shown that vehicles with aluminum bodies have a five-star safety rating.[57], [58].

In terms of durability, aluminum is completely recyclable. In terms of performance, lighter vehicles have a greater range and the power generated by the engine does not dissipate on the weight given by the movement of the vehicle, but is converted into energy for travel.

#### chassis

The chassis is the component on which all the other parts of the tricycle are placed and in its manufacture we went through the following stages:



Fig. 5.27 - Chassis

The fork is the component on which the drive wheel is mounted.



Fig. 5.28 - Assembly of the damping system

#### Rear axle

The rear axle is the component on which the two rear wheels are mounted.



Fig. 5.29 - Rear axle

Following the first tests, the central joint, which has the role of facilitating the inclination, gave way, as can be seen in the images below.

To solve this problem, the solution chosen was to mount the system at an angle of 45 degrees to the initial position, so that the walls of the wheel joint stiffen the center piece, thus avoiding its deformation.

Another way to stiffen the entire structure was to choose a profile with a thicker thickness, but this was not possible due to the fact that it was not available in the commercial version, and mounting between the two types of profiles was no longer possible.

**Table 5-6 - Technical specifications of the prototype IV**

Product features	Variant IV
	Wheel configuration
Inclined wheels	3
Frame built of	aluminum
Maximum passenger weight	150 kg
Full speed	30 km / h
Autonomy	25 km
Battery	36v 10mA lithium ion
Charging time	2 hours
Weight	22 kg
Dimensions (L x W x H) mm	500x660x760 (Folded)
	930x600x1250
Actuating power	250 W
Wheel size	12 "
Price	8500 lei

### 5.2.5. Stage V

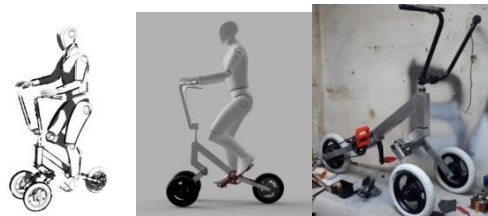


**Fig. 5.30 - Sketches stage V**

It was considered to change the grounding solution as follows: two wheels on the front and one wheel on the back.

This change involved a design and design effort, but following the tests performed for a tricycle with the driver's position, the use of this support solution is much more efficient.

The adoption of this solution also allowed the installation of a pedal block that ensures greater independence, stability and increased safety for the user / driver.

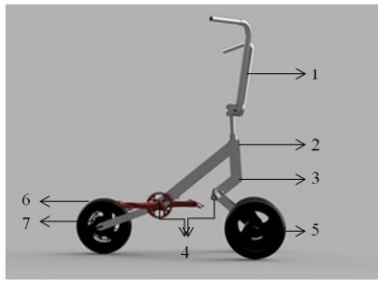
Thus, the developed three-wheeled vehicle contains structural materials to reduce costs and be easier to assemble, using standard technologies.

The structural materials used for the test are AISI 1060 steel and an aluminum alloy to reduce the weight of the vehicle.

This system was originally designed for urban areas, if the surfaces are flat, where the typical autonomy of the three-wheel electric vehicle is sufficient, but also the applicability of this vehicle can be extended by a suspension system.

Development of the electric vehicle with 2F1S

For the development of this three-wheeled electric vehicle, the following objectives were set: foldable and light storage, the existence of a compact suspension system, adaptability for different terrain inclinations.



1. The handlebars
2. The frame
3. Fork
4. Damping system
5. Driven wheel
6. Wheel
7. The engine

#### Folding system

The development of the 2F1S electric vehicle folding system takes into account two main factors: the adjustment of the vertical position using a circular profile and the shape of the handlebar, which can be adjusted and set on a vertical axis (position), with an inclination of up to 120°. This position can be secured using a clamping device.

This folding system offers a reduction in height of up to 50%, 870 x 750 x 618 mm, half the initial height (1240 mm).

#### Damping system

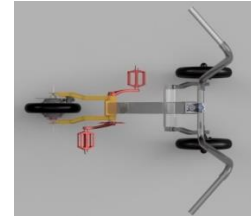
The suspension system contains 4 elastomeric elements fixed between two polygonal profiles. This type of suspension is used in the automotive industry, due to its low weight compared to the classic system of springs and shock absorbers.



Damping system



Chassis



Rear axle

**Fig. 5.31** - components

The driven wheels can change their position independently, which ensures movement on different surfaces, with different inclination for the vehicle.

**Table 5-7** - Technical specifications of the prototype IV

Product features	
	Variant V
Wheel configuration	2R1S
Inclined wheels	3
Frame built of	aluminum
Maximum passenger weight	150 kg
Full speed	30 km / h
Autonomy	25 km
Battery	36v 10mA lithium ion
Charging time	2 hours
Weight	22 kg
Dimensions (L x W x H) mm	618x660x760 (Folded)
	1150x600x1250
Actuating power	250 W
Wheel size	12 "
Price	9000 lei

## Chapter 6. Experimental determinations for the validation of the innovative five-stage design algorithm

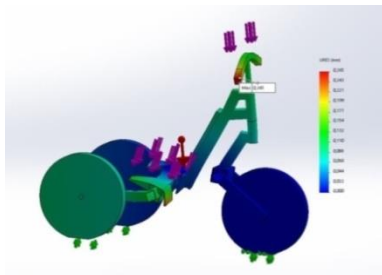
### 6.1. Analysis of the behavior of the steel frame using the finite element method

A study was performed using the finite element method using the Solid Works program with a force having a value and 2850 N. This force is twice the maximum force that can appear in the system corresponding to the case of the maximum load of the tricycle.

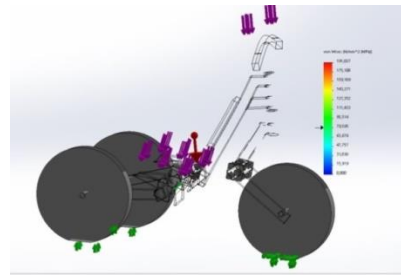
Successive simulations of the tricycle structure were performed, comprising all the components of the tricycle.

The purpose of the simulation was to validate, in terms of strength, the shape of the model and the designed design, in the conditions of demand with maximum values of external forces represented, in fact, by the user.

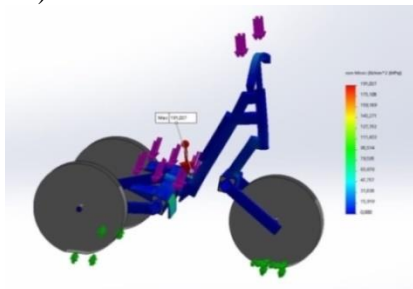
Loading 2850 N



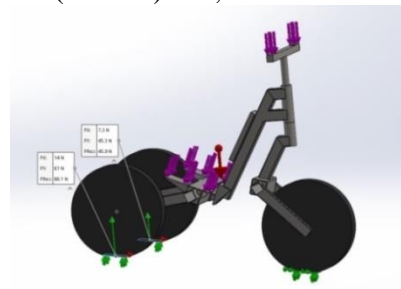
Steel 295 deformation at 2850 N  
Ures (mm) max 0.265



Steel 295 Iso 2850 N  
Von Mises (N / mm) 191,027



Steel 295 voltage at 2850 N  
Von Mises (N / mm) 191,027



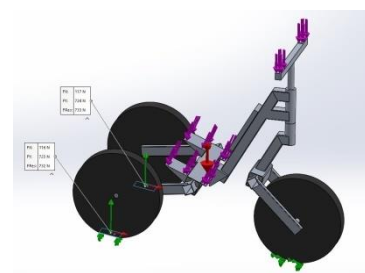
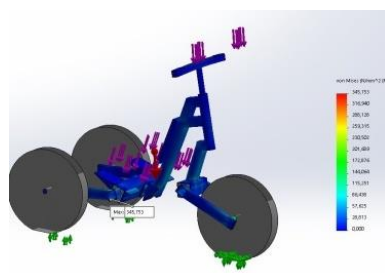
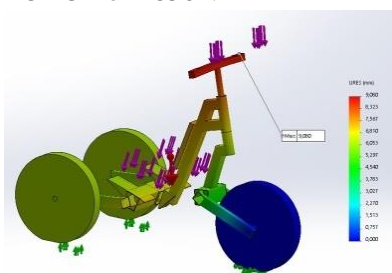
Rear reaction at 2850 N

**Fig. 6.1 - Finished steel analysis 295**

### 6.2. Finite element analysis of the aluminum frame

Due to the similarities between the framework studies, its simulation was also illustrated by changing only the material used (AL 6080), the simulation results being highlighted below. The values with which the frame was loaded are the same as in the study with Steel 295.

Aluminum AL 6080 iso force 320 N  
FORCE of 2850N



Frame deformation AL 6080 at 2850N	Frame voltages AL 6080 to 2850N	Rear frame reactions AL 6080 to 2850N
Ures (mm) max 9,060	Von Mises (N / mm) 345,153	

**Fig. 6.2** - Finite element analysis of the AL 6080 aluminum frame

The designed components withstand the stresses and loads during the use of the tricycle, representing a functional, robust and efficient assembly.

In component design, load values were considered to have maximum values. Therefore, the resulting dimensions are significantly larger than the minimum values required for the operation of the tricycle. The simulations show a slight oversizing of the frame dimensions, values that will be changed later.

The designed components require an optimization that leads to the reduction of production costs and the weight of the tricycle, in the conditions of adopting an appropriate, innovative design.

### 6.3. Research on the determination of displacements using tensometric transducers



**Fig. 6.3** - Tensometric transducers and the adhesive used

Electrical tensometry is the method of measuring the deformations and elongations of a required body, by means of transducers that transform variations of mechanical deformations into variations of an electrical quantity.

Electrical tensometry is part of the general methods of electrically measuring electrical quantities [59] [60].

Operating principle of the resistive transducer.

The transducer is glued on the piece under investigation so as to faithfully follow its deformations. It was found that the specific variation of the resistance of the transducer is, within certain limits, practically proportional to the specific deformation suffered by the part on which the transducer is applied.

A superglue Z70 adhesive will be used to apply the sensors for measurement, following the manufacturer's instructions.

Superglue Z70 is used for cold hardening for experimental tests and for sensors without high precision requirements.

It has an extremely fast curing time of only one minute at 20 ° C, the superglue Z70 being commonly used in many experimental test loads for gauge installation. This cyanoacrylate adhesive is also used in the manufacture of sensors, although usually only if high precision is not required.

Z70 can only be cleaned in very thin adhesive layers. As the humidity absorbed by the ambient air serves as a catalyst, the relative humidity should be about 40-70%. Treatment with cyanoacrylates and, consequently, Z70 also depends on the chemical state of the adhesive surface.

If the application conditions are unfavorable (eg relatively low humidity, acid reaction surfaces, low temperatures), the additional use of the BCY01 accelerator is recommended. A

drop of this accelerator can be applied to the adhesive surface. After about a minute, superglue Z70 can be applied.

Cold cleaning of the upper surface: It hardens very quickly under the pressure of the thumb (0.5 minutes at 30 ° C / 1 ° C, 1 minute at 20 ° C, 10 minutes at 5 ° C / 41 ° F).

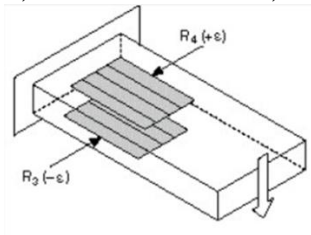


**Fig. 6.4 - Positioning of tensometric marks[61]**

The tensometric marks were mounted on the rear axle arms and on the fork arms at a distance of 60 mm from the end of the arm and positioned in parallel on the upper and lower part of the profile.

For each measuring point two tensometric marks connected in a semi-bridge were used. For the measurements carried out in the laboratory, a data acquisition system based on NI6281 cDAQ-9171 USB cards was used together with the SCM 5b38 signal conditioners and the NI 9215 module from DataForth. NI 9191 WiFi acquisition board and NI 9215 module were used for outdoor measurements.

Measuring devices:



**Fig. 6.5 - Measuring devices**

#### 6.4. Measuring the stiffness of the steel arm

To measure the stiffness of the arm subjected to a torsion, it was mounted on a rigid system that can move vertically. By fixing the end of the arm to a fixed landmark and moving it vertically, the loading force of the system was obtained. Fig. 6.7.



**Fig. 6.6 - Measuring the stiffness of the steel arm without joint**

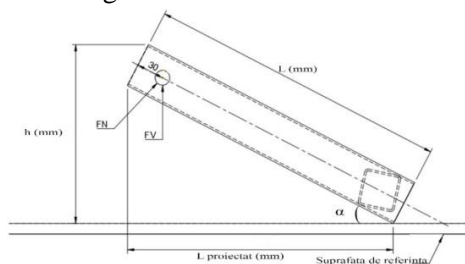


**Fig. 6.7 - Scheme of arm stiffness measurement**

The mass of the counterweights was determined using a precision scale, and the force applied to the structure was obtained by calculation. Fig. 6.7 relationships:

$$\sin \alpha = \frac{h}{L} \rightarrow \alpha = \arcsin \frac{h}{L} \quad 6-1$$

$$h = L \cdot \sin \alpha \quad 6-2$$

$$F_v \cos \alpha = \frac{F_N}{F_v} \quad 6-3$$

$$F_N = F_v \cdot \cos \alpha \quad 6-4$$

$$M = F_N \cdot L \quad 6-5$$

The calculated sizes, depending on the vertical movement of the arm subjected to forceful stress were, the angle of inclination and the bending stresses.

The stresses to which the steel bridge arm is subjected were calculated with the relationship 6-6. The graphical representation of this function is in Fig. 6.8. The square of the correlation coefficient is  $R^2 = 0.995$ .

$$T = 6133 \cdot 0,023F - 0,325dh + 10^{-3} + 0,205dh^2 + 4,8610 \cdot 5F^2 - 6,50910 \cdot 3Fdh \dots \quad 6-6$$

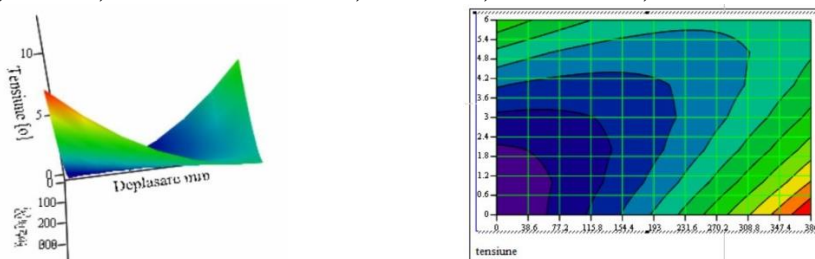


Fig. 6.8- Graphical representation of the angle of inclination of the applied force and the displacement

The inclination to which the steel bridge arm is subjected has been calculated with the relation 6-7. The graphical representation of this function is in Fig. 6.9. The square of the correlation coefficient is  $R^2 = 1$ .

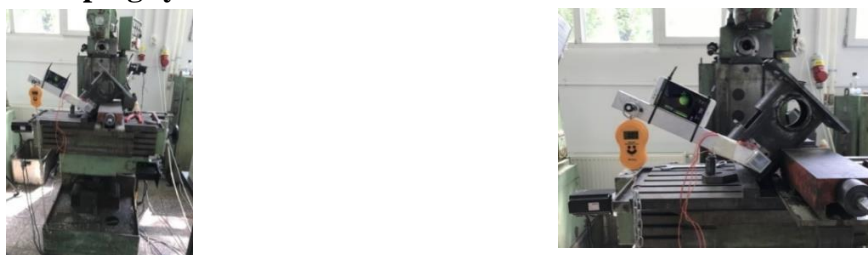
$$\alpha = 28,001 - 2,21210 \cdot 3F + 0,059dh - 9,71310 \cdot 6F^2 + 1,50810 \cdot 3 - 0,057dh^2 \dots \quad F \cdot dh \quad 6-7$$



Fig. 6.9 -Graphical representation of the applied inclination tension and displacement

The graphs obtained in the figure Fig. 6.8 and Fig. 6.9 are obtained with the MathCad program.

### 6.5. Measurements with tensometric transducers on the steel rear axle arm, with elastic damping system



**Fig. 6.10** - Measurements using tensometric transducers for aluminum rear axle arms without elastic damping system

The calculated sizes, depending on the vertical movement of the arm subjected to forceful stress were, the angle of inclination and the bending stresses. The stresses to which the aluminum bridge arm is subjected were calculated with the relationship 6-8. The graphical representation of this function is in Fig. 6.11. The square of the correlation coefficient is  $R^2 = 0.999$ .

$$T = -0.043 + 0.025 \cdot F + 0,407 \cdot dh - 1,4881 \cdot 10^{-4} \cdot 0,016Fdh + F^2 + 0,295dh^2 \quad 6-8$$

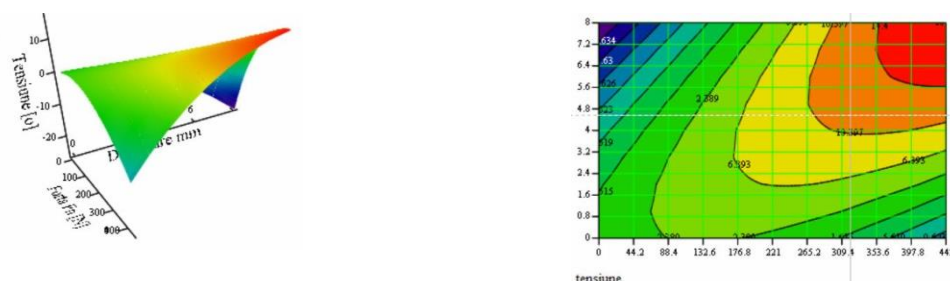


**Fig. 6.11**- Graphical representation of the angle of inclination depending on the applied force and the displacement

The stresses to which the aluminum bridge arm is subjected were calculated with the relationship 6-9. The graphical representation of this function is in Fig. 6.12. The square of the correlation coefficient is  $R^2 = 0.989$ .

$$\alpha = 26,301 - 791610 - 4F - 0,012dh + 174610 - 4Fdh - 0.0222 \cdot 2,19810 - 6F^2 \dots \dots \dots \quad 6-9$$

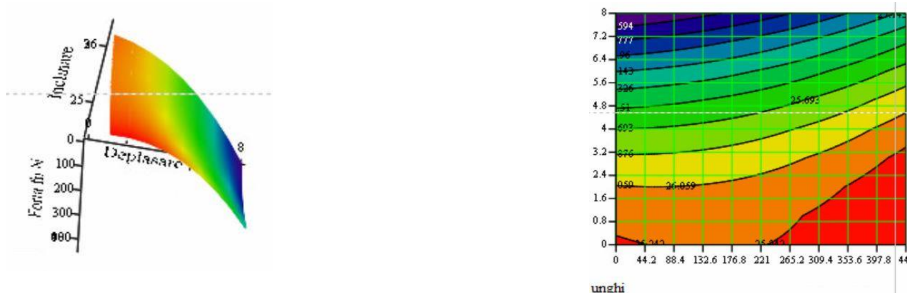


**Fig. 6.12** -Graphical representation of the inclination stresses as a function of the applied stress and the displacement

The graphs obtained in Fig. 6.11 and Fig. 6.12 are obtained with the Math-Cad program

### 6.6. Measurements with tensometric transducers on the steel rear axle arm, with elastic damping system

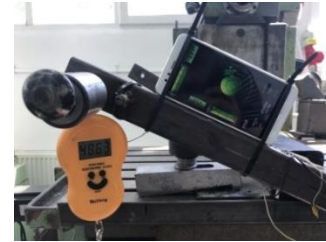
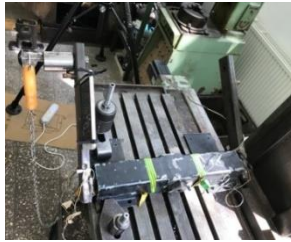
From the graphs presented it can be seen that the maximum stress reached is 5.5 MPa resulting from the application of a force of 385.74 N on the non-damping steel arm fixed at one end. The addition of an elastic joint under the same conditions results in the maximum



measured measured tension being 5.2 MPa resulting from the application of a force of 425.55 N.



Rear axle mounted on the workbench;



A force of 425.555 N was applied and an angle of 26.8 degrees was generated

**Fig. 6.13** - Measurements using tensometric transducers for the rear axle arms with elastic damping system

Given the fact that the steel arm with damping system supports a higher load than an arm without damping system we can say that when using the proposed damping system the metal structure can be resized.

The calculated sizes, depending on the vertical movement of the arm subjected to the force were, the angle of inclination and the bending stresses. The stresses to which the steel axle arm with elastic articulation system is subjected were calculated with the relation 6-10. The graphical representation of this function is in Fig. 6.14. The square of the correlation coefficient is  $R^2 = 0.998$ .

$$T = 28.78 + 0.144F + 1.759 \cdot 2,128.10 - 3F^2 + 0.05Fdh - 0.295dh^2 \dots \dots \quad 6-10$$

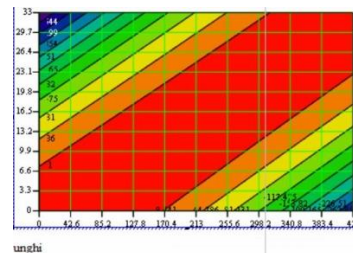
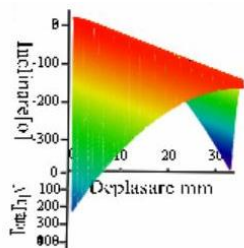


**Fig. 6.14** - Graphical representation of the inclination angle as a function of the applied force and the displacement

The stresses to which the aluminum bridge arm is subjected were calculated with the relationship 6-11. The graphical representation of this function is in Fig. 6.15. The square of the correlation coefficient is  $R^2 = 0.999$ .

$$\alpha = 0.214 + 0.028F + 7.92210 - 3dh - 8.722610 - 5F^2 + 1.03610 - 3Fdh - 2.92510 - 3dh^2 \dots \dots \quad 6-11$$

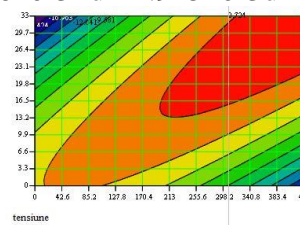
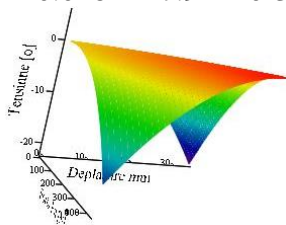


**Fig. 6.15** - Graphical representation of the inclination stresses as a function of the applied stress and the displacement

The graphs obtained in Fig. 6.14 and Fig. 6.15 are obtained with the MathCad program.

### 6.7. Measurements with tensometric transducers on the aluminum rear axle arm, with elastic damping system

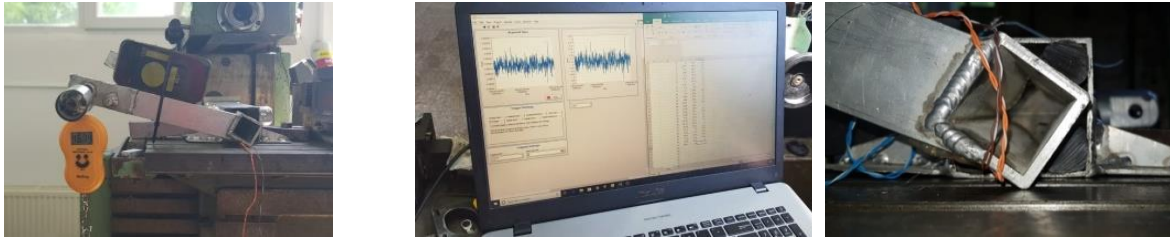


**Fig. 6.16** - Aluminum articulated arm with elastic damping system

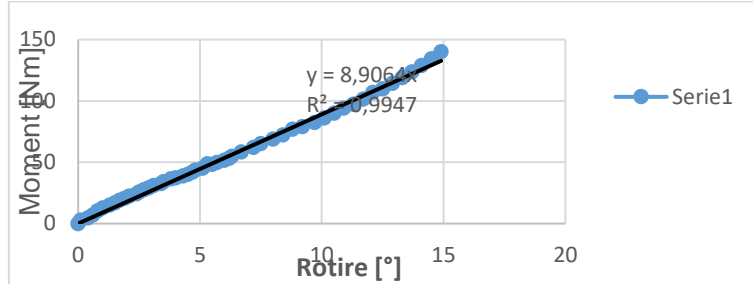


**Fig. 6.17** - Stiffness of the aluminum arm with articulation on the load

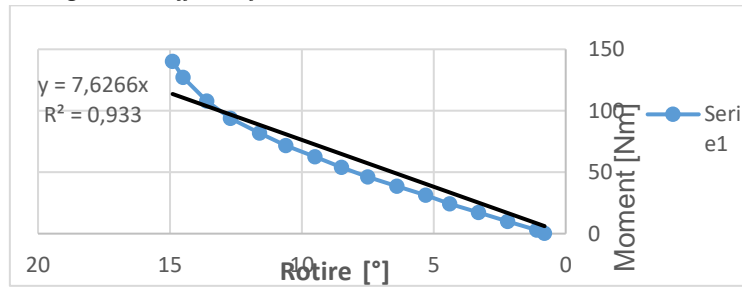


**Fig. 6.18** - Stiffness of the aluminum arm with articulation on discharge

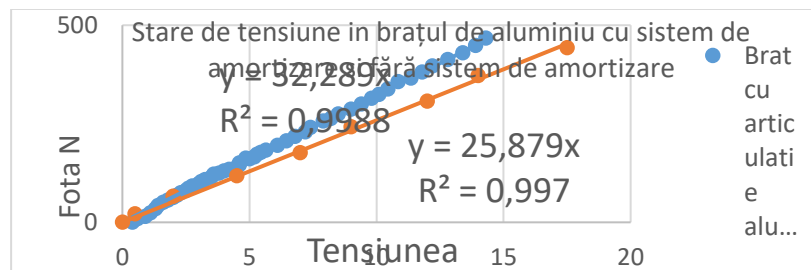


**Fig. 6.19** - Tensions in the articulated arm and the articulated arm

In the Fig. 6.19 the maximum reached stress of 17.5 MPa can be observed resulting from the application of a force of 442.452 N on the aluminum arm without joint fixed at one end. By adding an elastic joint under the same conditions it results that the maximum measured measured stress is 14.3 MPa. Resulting by applying a force of 467.27 N.

Given that the aluminum arm with damping system supports a higher load than an arm without damping system we can say that when using the proposed damping system the metal structure can be resized in the direction of dimensional reduction reducing dimensions we reduce the weight of the whole cost with materials and at the same time increase the autonomy of the tricycle.

The calculated quantities were the angle of inclination and the bending stresses. The inclination to which the aluminum bridge arm with elastic joint system is subjected were calculated with the relation 5-12. The obtained equation is valid for the travel range between 0 and 72 mm. The graphical representation of this function is inFig. 6.20. The square of the

correlation coefficient is  $R^2 = 0.966$ .

$$T = 28.78 + 0.144F + 1.759 \cdot 10^{-3}F^2 + 0.05Fdh - 0.295dh^2 \dots\dots$$

6-12



Fig. 6.20 - Graphical representation of the inclination angle as a function of the applied force and the displacement

The tension to which the aluminum bridge arm with elastic joint system is subjected were calculated with the relation 6-13. The obtained equation is valid for the travel range between 0 and 72 mm. The graphical representation of this function is in Fig. 6.21. The square of the correlation coefficient is  $R^2 = 0.999$ .

$$\alpha = 0.214 + 0.028F + 7.922 \cdot 10^{-3}dh - 8.7226 \cdot 10^{-5}F^2 + 1.0361 \cdot 10^{-3}Fdh - 2.925 \cdot 10^{-3}dh^2 \dots\dots$$

6-13



Fig. 6.21-Graphical representation of the inclination stresses as a function of the applied stress and the displacement

The graphs obtained in Fig. 6.20 and Fig. 6.21 are obtained with the MathCad program

#### Conclusion

Following the experimental tests performed by 10 users with different weights, they mentioned as the main advantage of the structure with elastic damping made of rubber, compared to elastic systems with spring damping or hydraulic piston that they feel less pressure transmitted through the structure tricycle to the spine.

In the version of the frame with suspension system can be seen in Fig. 6.19 a higher degree of resistance to a lower voltage resulting in the shocks being taken over by the damping system. The analyzed 490 Nm force corresponds to a user with an average weight halved.

The thickness of the chosen profile generated very low stresses resulting in the fact that the profile is oversized and can be subjected to a higher load or can be resized to reduce the total weight, implicitly the manufacturing price.

Analyzing the graph, the force (generated by the mass with which it was requested) together with the state of stresses measured on the entire variation level, it is found that the voltage in the damped frame is lower than the voltage in the damped frame.

#### Conclusion

Following the experimental tests performed by 10 users with different weights, they mentioned as the main advantage of the structure with elastic damping made of rubber, compared to elastic systems with spring damping or hydraulic piston that they feel less pressure transmitted through the structure tricycle to the spine.

In the version of the frame with suspension system can be seen in Fig. 6.19 a higher degree of resistance to a lower voltage resulting in the shocks being taken over by the damping system. The analyzed 490 Nm force corresponds to a user with an average weight halved.

The thickness of the chosen profile generated very low stresses resulting in the fact that the profile is oversized and can be subjected to a higher load or can be resized to reduce the total weight, implicitly the manufacturing price.

Analyzing the graph, the force (generated by the mass with which it was requested) together with the state of stresses measured on the entire variation level, it is found that the voltage in the damped frame is lower than the voltage in the damped frame.

As a result of these results it can be concluded that in the case of the arm provided with damping we can reduce the dimensions of its cross section (either length, width or thickness) which leads to a reduction in the weight of the arm resulting in a positive impact:

- reduction of manufacturing cost;
- reducing the Co2 footprint of the newly manufactured product as well as in the recycling stage;
- weight reduction;
- increasing the autonomy offering the possibility to use a smaller battery.

### 6.8. Research on weight distribution on tricycle wheels

In order to determine the load values of the tricycle under the weight of the user in operation, use scenarios were created, of which one scenario with the frame without load taken as reference and three scenarios with the frame under user weight, on braking, left turn and right turn . Three identical calibrated scales, positioned under each wheel of the tricycle, were used to perform the measurements.

From the distribution of the frame's own weight together with the adjacent components with a value of 32 Kg in total, it resulted that 17 Kg are distributed on the front axle and 7.5 Kg on each arm on the rear axle.

In the use scenario, in which an average user weight of 106 Kg and a tricycle weight of 32 Kg are taken into account, the distribution of the total weight at rest was as follows: front axle 54.6 Kg and rear axle 41.7 Kg on each arm.

In the braking scenario the distribution of the total weight was: front axle 72.8 Kg and rear axle 32.6 Kg on each arm.

In the use scenario in which the tricycle is on the turn, the weight distribution was as follows: front axle 48 Kg and on the rear axle on the arm inside the turn 71.2 Kg and on the arm outside the turn 18.8 Kg.

The results contributed to the optimization of the tricycle frame regarding the finite element analysis providing the necessary parameters for the mechanical loading of the tricycle and its constraint in the static tests.

### 6.9. Measurements with resistive transducers in conditions of ascent and descent of the user

The stages of performing the experiment

To carry out the experiment, an articulated frame was used on which resistive transducers were mounted on the fork arms and on the rear axle arms subsequently connected to the measuring device used, the NI 9191 WiFi acquisition board and the NI 9215 module.

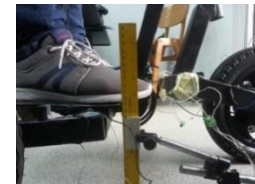
On the articulated tricycle, user climbing tests with different weights were performed to observe the highest tensions.



The height of the rear axle with a load of 44 kg is 204 mm



The height of the rear axle with a load of 77 kg is 190 mm



The height of the rear axle with a load of 104 kg is 188 mm

Fig. 6.22 - Dynamic measurements with user ascent and descent

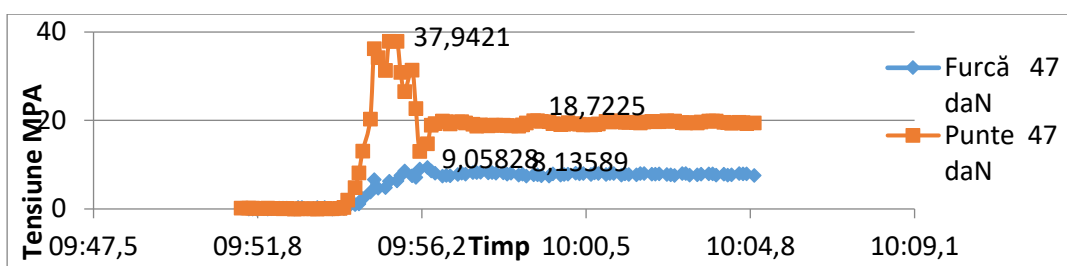


Fig. 6.23 - frame loads with a value of 47 daN

At the time of loading the frame with the value of 47 daN the maximum tension on the rear axle arm was 37.9 MPa while on the front axle it was 9.05 MPa after which the values stabilized at 18.72 MPa respectively 8, 13 MPa. The maximum voltage was reached over a period of 2 milliseconds.

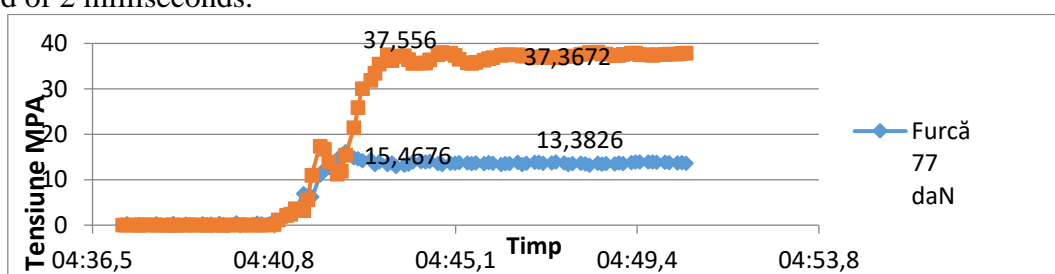


Fig. 6.24 - Loading the frame with the value of 77 daN

At the time of loading the frame with the value of 77 daN the maximum tension on the rear axle arm was 37.55 MPa while on the front axle it was 15.46 MPa after which the values stabilized at 37.36 MPa respectively 13, 38 MPa. The maximum voltage was reached over a period of 4 milliseconds.

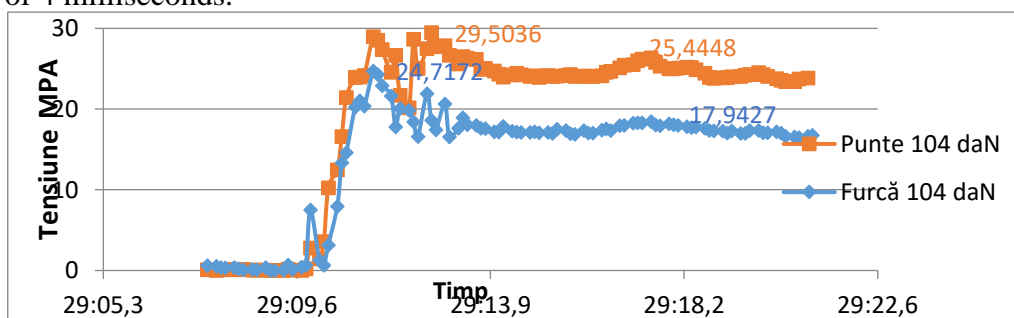


Fig. 6.25 - loading the frame with the value of 104 daN

At the time of loading the frame with the value of 104 daN the maximum tension on the rear axle arm was 29.50 MPa while on the front axle it was 24.71 MPa after which the values stabilized at 25.44 MPa respectively 17, 94 MPa. The maximum voltage was reached over a period of 7 milliseconds.

### 6.10. Dynamic study with overcoming obstacles

The dynamic study was performed using two tensometric transducers on each arm (rear axle and fork) in the lower and upper arm, using a WiFi acquisition board NI 9191 and module NI 9215. The loading of the tricycle under normal operating conditions with a medium weight user (106 Kg) on the road with overcoming obstacles. The study shows that the shocks are taken over by the damping system and are not transmitted to the user, not affecting his spine. The images below show the results of the tricycle study at different loading stages. The load amplitudes are represented in graphs by colors assigned to each arm.

The tension state on the right and left rear axle in relation to the forward direction is highlighted in the following graphs by:

- red color = state of tension measured by tensometric marks mounted on the left rear arm;
- dark blue / white color = voltage state measured by tensometric marks mounted on the right rear arm;
- green color = state of tension measured by the tensometric marks mounted on the left arm of the front fork;
- light blue color = the state of tension measured by the tensometric marks mounted on the right arm of the front fork.



- No loading



- Leaving the place



- Riding the front wheel



- Lowering the obstacle with the front wheel



Climbing the obstacle with the rear wheels



h - Lowering the obstacle with all wheels

**Fig. 6.26** - Dynamic study with crossing the obstacle

In the images you can see the loading conditions of the tricycle when the user climbs and leaves, the loading conditions of the tricycle when crossing an obstacle with the front wheel the images can see the loading conditions of the tricycle when crossing an obstacle with the rear axle and its balancing / returning state being observed in the graphs below the period of oscillations.

Dynamic study with 360 ere return



a) The initial stage



b) Tilt on the turn



c) The return

**Fig. 6.27** - Dynamic study with 360 ° return

Images a, b, c show the loads that appeared in the situation of a complete turn (360 degrees). Higher amplitudes can be observed during the turn resulting from the pendulum effect compared to passing over obstacles. Loads are transferred to the side of the tricycle to the outside of the turn

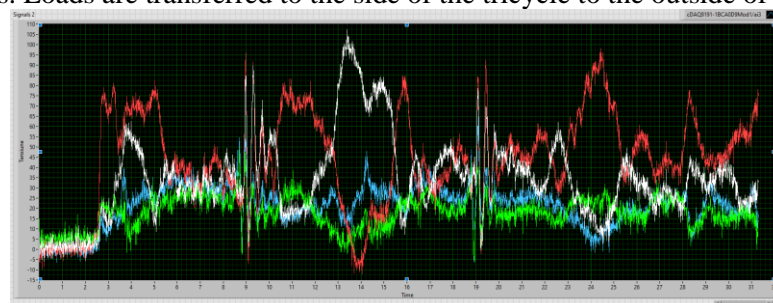


**Fig. 6.28** - Dynamic study chart with overcoming obstacle and 360° turn

In the graphs above you can see the dynamic behavior of the tricycle in different use scenarios with crossing the obstacle and turning 360 degrees under a constant weight of the user.

## Dynamic single-wheel obstacle course study



Fig. 6.29 - Dynamic study

In order to determine the integrity of the tricycle frame, studies were performed on crossing with one wheel. Multiple scenarios were studied regarding the accidental but also intentional impact of an obstacle in order to determine the stability of the tricycle and its maneuverability in extreme conditions of use. Studies show the amplitude of tensions in the environment following the operation of the tricycle in urban areas.

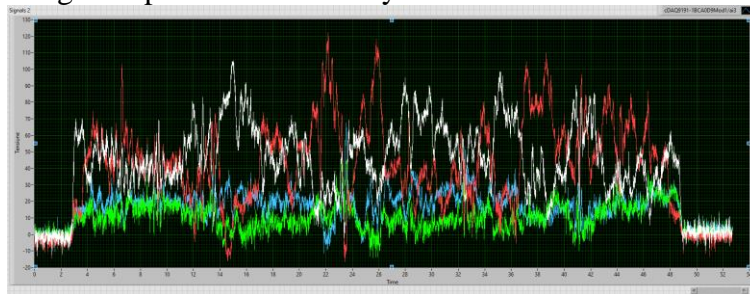


Fig. 6.30 - Dynamic study chart with single wheel obstacle crossing

## Dynamic study when descending a slope with unevenness.



Fig. 6.31 - Dynamic study when descending a slope with unevenness.

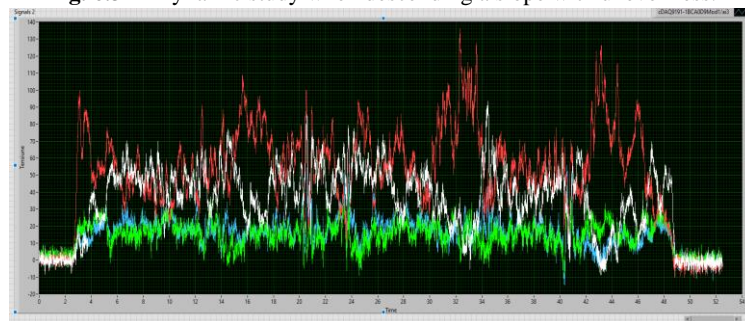


Fig. 6.32 - Dynamic study graph when descending a slope

The studies carried out above show that the use of the tricycle in the current geometry works correctly from the point of view of the suspension and inclination system, offering an ergonomic and safe use. The tests validate the need for a suspension and tilt system, providing a high degree of maneuverability and comfort for the user.

The behavior of the real prototype was slightly different from that of the virtual simulation, because, for the kinematic simulation, the 3D model was simplified, however, the prototype worked as expected (Chapter 4.51, Fig. 5.25)

## Chapter 7. Optimization algorithms by parametric resizing of the metal structure

In the models developed in the figures below, we tried to test the easiest optimization variant, by drilling a segment of the frame and testing using finite element analysis using the Solid Works / Simulation program to verify the structural integrity of the frame.

For the structural optimization of the frame, the Voronoi and Shape Generator technique was applied.

In the first stage, the forces acting on the tricycle frame were studied to generate the necessary conditions for the stability, strength and functionality of the whole system.

Once these are established, the constraints of the frame will be optimized by applying the Voronoi diagram. This applies at the part level.

A product designed parametrically with a minimum amount of material optimized and distributed in a functional way will be a product with a significantly reduced weight with a low production cost, and the shape it will take will be organic.

Two such products optimized by parametric design are a wheelchair for people with disabilities, and a motorcycle frame, both printed in 3D, with a custom structure on the user's dimensions, offering a much higher degree of comfort than the classic ones.

Modern design methods are increasingly based on understanding the nature of processes and the principles of automatic organization of biological structures, their representation being made by technological methods based on mathematical models, methods most often used in contemporary architecture.

Bionic design elements play a very important role in urban modeling and development, from architecture to product design. The development of information technology has made it possible to create more complex structures inspired by natural forms. The Voronoi diagram had as a model for relaxing the surface, the structure of the honeycomb or the wing of the dragonfly, ( Fig. 7.1 a B C).

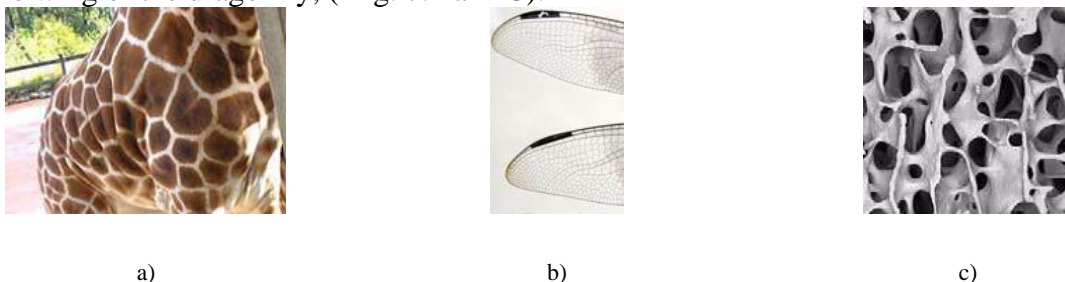


**Fig. 7.1** - Examples of biological structures that use automatic organization. [62]

In mathematics, a Voronoi diagram is a partitioning of a plane into regions based on a distance to the points in a specific subset of the plane. This set of points (called seeds, sites or generators) is specified in advance, and for each point, there is a corresponding region consisting of all the points closest to it than any other. These regions are called Voronoi cells. The Voronoi diagram of a set of points is double its Delaunay triangle.

A weighted Voronoi diagram is one in which the function of a pair of points to define a Voronoi cell is a function of distance modified by multiplicative or additive weights assigned to the generating points, In contrast to Voronoi cells defined using a distance that is a metric, in this case, some of the Voronoi cells may be empty. A power diagram is a type of Voronoi diagram defined from a set of circles that uses power distance; it can also be thought of as a weighted Voronoi diagram in which a weight defined by the radius of each circle is added to a square distance from the center of the circle [63] [64].



Parametric design is a process based on an algorithmic thinking model that facilitates the expression of parameters and rules that together can decode or clarify the relationship between response / result and the initially proposed design,

In essence, parametric design is a paradigm in the field of modern creation, in which the relationship between elements is used to model the design of complex geometric elements and structures.

The term "parametric" is commonly used in mathematics and refers to the use of certain variables that can solve or constrain the results of an equation.

All these applications that combine clear mathematical formulas and specific constraints in the design of a piece or assembly, facilitate the whole design process. The initial data about the total size, the shape of a profile and then the application of one of the two variants Voronoi or parametric design provides an optimization of the shape superior to the classic design methods and implicitly, the design

Starting from the above examples, the two optimization techniques were applied on the tricycle, respecting the initial shape and functionality.

### 7.1. Topological conceptual optimization of the framework

For the problems found in balancing the distribution of internal stresses and optimizing the structure, solutions can be found in the forms proposed by nature [65].

The cells divide the space so that, under minimal structural constructive efforts for the body, the balance of internal effort distributions, the optimization of flows for different forms of energy transport, creates the optimization of the route of an information circuit.

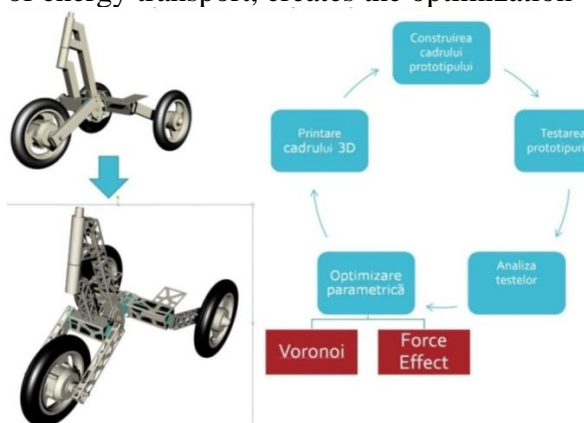


Fig. 7.2 -Frame optimization [66]

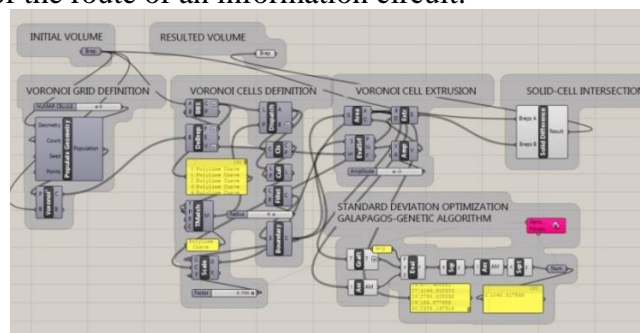
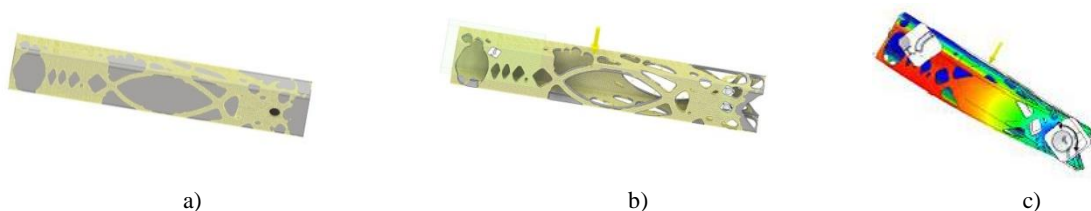


Fig. 7.3. - Network generated with the Grasshopper program[66]

Given these considerations, the frame was optimized using the Voronoi method, thus reducing the amount of material without affecting its strength. The Rhino program was used in conjunction with the Grasshopper plug-in, generating a network that selected certain criteria to consider, given the ratio of forces generated previously, (Fig. 7.3).

This image shows the definition used to create the Voronoi grid and set the full-blank ratio. Genetic algorithms have been used to produce close-surface cells.

To test a component of the assembly with the vortex grid applied, the component was imported into the Inventor and forces were applied to assess the strength of the component, as exemplified below. in the Fig. 7.4, Fig. 7.5, Fig. 7.6 and Fig. 7.7.



**Fig. 7.4** - The optimization process for a component of the framework

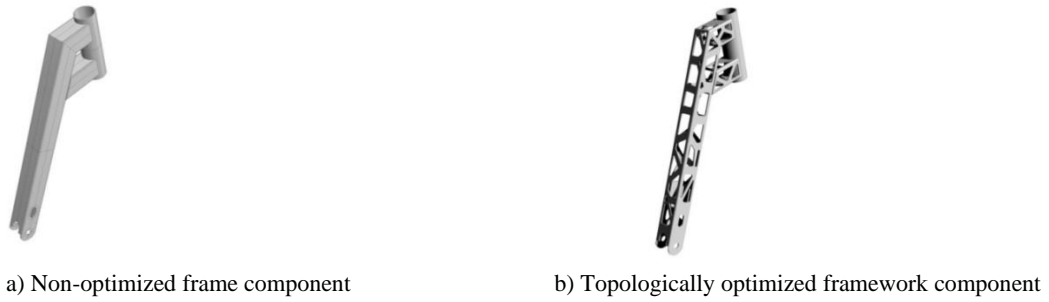


**Fig. 7.5** - Tricycle frame, a) before optimization, b) after optimization

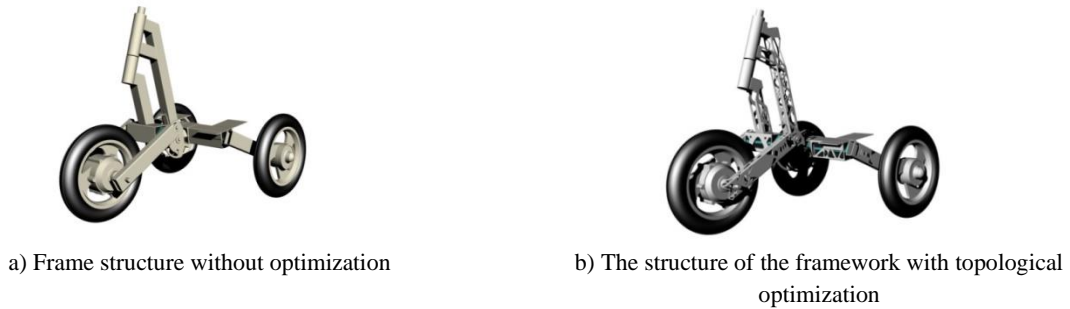


**Fig. 7.6** - Tricycle frame before and after topological optimization

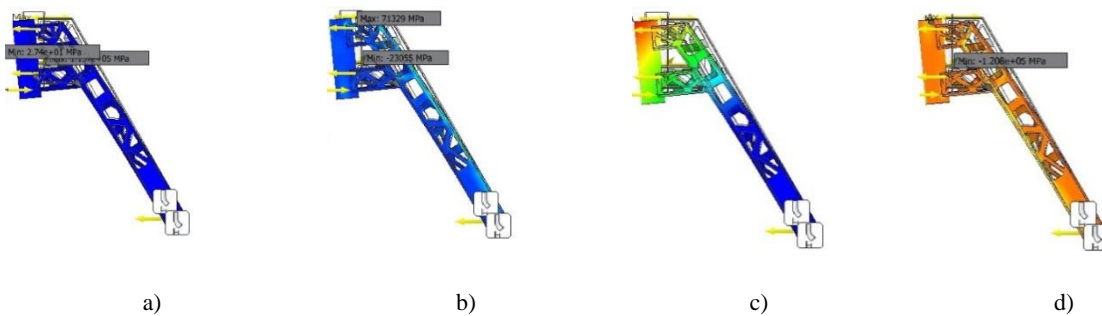


**Fig. 7.7** - The tricycle frame during the optimization process

The forces distributed in each region are represented in Fig. 7.7.

To apply Shape Generator, the Inventor program was used to build the frame and select mobile, fixed, and distributed forces in Force Effect. Using Shape Generator resulted in a discretization that was used as a template to cut the original part, as shown in Fig. 7.7.

### Conclusions

Following these studies, the use of the two optimization methods using parametric design to improve a metal structure can lead to an object with superior mechanical and aesthetic characteristics but with much higher production costs.

Using these optimization processes streamlines the design, production and testing methods, reducing the time required to achieve them, eliminating human error in the process. These methods of product optimization can be approached at a practical level only with the decrease of the costs of the technological processes necessary for its manufacture.

### 7.2. Theoretical optimization of the 2F1S framework

The frame optimization was done in the CAD program Fusion 360 from AutoDesk, in the simulation module “Simulation / Shape Optimization”. The optimization process is similar to that of the study of forces regarding the constraint elements (material, fastening system). The optimization of the 3D model is performed by fulfilling two global objectives, which justifies the phenomenon by which an object increases its safety factor (it is stiffened) while its mass decreases. [67]. These overall objectives are “Target Mass” and “Rigidity” and are defined before the start of the study.



**Fig. 7.8** - Frame 2F1S

The target mass limits the mass of the optimized shape to a specified value, which is a percentage of the initial mass. The expression indicates that the resulting mass should be less than or equal to the specified value. High-resolution discretization should allow optimized geometry to reach the target mass in the 3-5% range.

**Stiffness.** The software maximizes the resulting 3D model rigidity based on structural constraints and applied loads. The mass is reduced by removing the elements from the areas that have the least impact on the rigidity of the model. The optimum stiffness to mass ratio is obtained, allowing the 3D model to have as low a mass as possible for the scope.

The default global objectives instruct the solver to produce a shape that maximizes the rigidity of the part while limiting the 3D model to 30% of the original mass.

Achieving these objectives achieves an optimized topology that removes material from areas where mechanical stress is minimal and does not have a negative impact on the integrity of the 3D model, while creating new geometries in the areas of discharge of mechanical stress, able to take the tasks the 3D model will be subjected.

After establishing the constraints, the optimization criteria for achieving an optimal weight and an ideal shape were applied, under the given conditions of application and for a chosen material.

Before starting the optimization process, you can use the "Simplify" module to make changes specific to the model, in order to simplify it, thus streamlining the optimization process. It eliminates unnecessary features that complicate the analysis and does not provide useful information. You can opt for the "Symmetry" command, when necessary, to reduce the size of the simulation model and the resolution time. Symmetry can also facilitate the constraint of a model in a way that ensures full stability, but does not prevent natural deformation.

The optimization process began by simplifying the original model, creating a full volume, keeping the fixing points and the physical proportions of the concept.

With this method, the program can indicate the specific areas of force distribution over a large area. This eliminates the constraints imposed by the shape of the original model, allowing the optimization process to choose an optimal topology for designing the structure of the tricycle.

The optimization of the shape of the structure had the following stages:

- the program indicates the areas that can be modified,
- the designer, depending on the result of the simulations, establishes the morphological form of the product.

The main component of the three-wheel electric vehicle system is the frame. For tests it is heavily loaded, to ensure the role of folding, suspension and movement on different surfaces. The frame must be light enough to be transported. The ideal weight for the frame is under 4 Kg. aluminum alloy and carbon steel. This type of material increases the resistance to mechanical stress, over time, for constant or variable loads.

These materials also offer already known assembly solutions, which offer an advantage of not losing material in unsuccessful assembly attempts.

Therefore, the main advantages in the use of structural materials are the assembly "know-how" technique and ecological criteria, using (common) resources in an innovative and intelligent way. The mechanical properties of the materials are presented in Table 7-1.

**Table 7-1** - Mechanical properties of materials

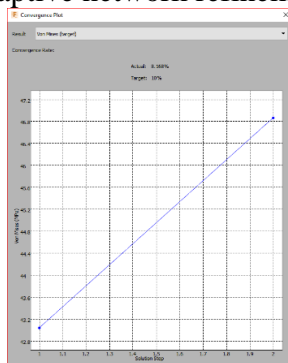
Density	7.85E-06 kg / mm <sup>3</sup>	Density	2.67E-06 kg / mm <sup>3</sup>
Young's Modulus	204773 MPa	Young's Modulus	71000 MPa
Poisson's Ratio	0.29	Poisson's Ratio	0.33
Yield Strength	372.3 MPa	Yield Strength	240 MPa
Ultimate Tensile Strength	512.3 MPa	Ultimate Tensile Strength	460 MPa
Thermal Conductivity	0.045 W / (mm C)	Thermal Conductivity	0.165 W / (mm C)
Thermal Expansion Coefficient	1.172E-05 / C	Thermal Expansion Coefficient	2.1E-05 / C
Specific Heat	480 J / (kg C)	Specific Heat	880 J / (kg C)

a) AISI 1061 steel

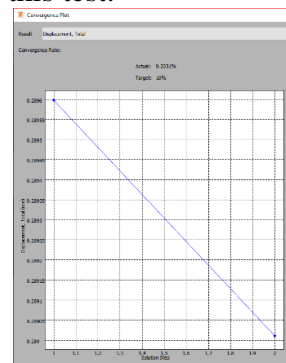
b) AlSiMg

To optimize the frame, various static stress tests were performed in the Fusion 360, using the Nastran solver, to check the total weight and that the vehicle withstands the forces applied when used. The weight of the frame plays a key role in the development of the final product. The vehicle must be light enough to be lifted and transported in various spaces, but also strong enough to carry out the task at hand.

The first test was performed using AISI 1061 steel as the frame material, as it is a common structural steel and also cost effective. In order for the static stress test, using the finite element method, to be valid, a convergence analysis was performed, presented in Table 7-1. An adaptive network refinement strategy was used for this test.



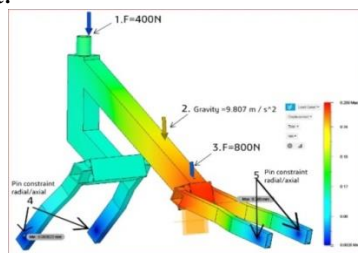
a) Von Mises



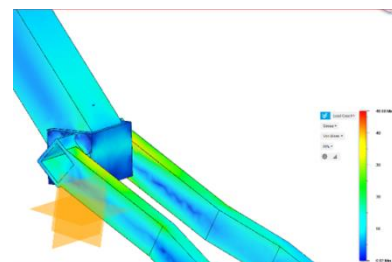
b) Travel 4

**Fig. 7.9.** - Convergence study, static stress Steel AISI 1061

The conditions applied for the study are presented in Fig. 7.10 and the finite element method was used to validate the solutions. The minimum safety factor resulting from the simulation was 7.94 for AISI 1061 steel, with a load of 1200 N applied to the frame (simulating the maximum load for a fully equipped adult user). The maximum deformation per frame was 0.289 mm. This result shows that the frame overload with a total weight of 10.86 kg. The current weight of the frame states that the vehicle is not easy to use for transport.



a) Forces and constraints on the frame



b) The stress areas of the main frame

**Fig. 7.10** - Study conditions

To reduce the weight of the steel frame, a topological optimization was approached. The optimization process followed the same steps as the static test with the added optimization criteria, low weight and maximizing the rigidity of the frame. The resulting topological optimization is presented in Fig. 7.11. The software allowed a small weight reduction of the frame from 10.86 Kg to 9.95 Kg, insufficient for the target weight of the frame.

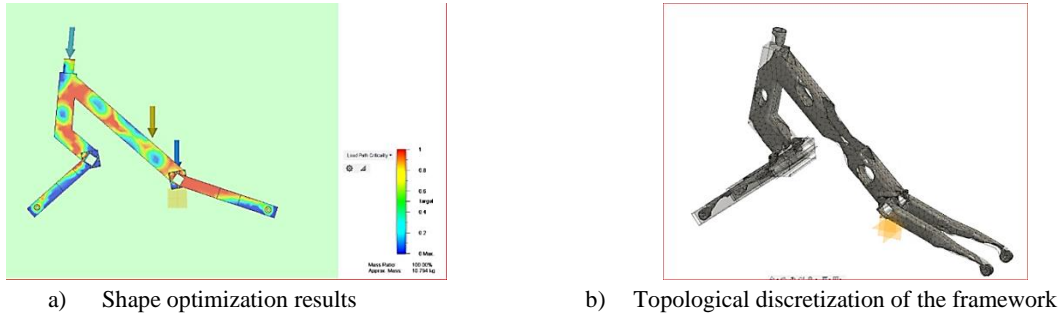


**Fig. 7.11** - The process of shape optimization

To achieve the target weight, but still maintaining its structural integrity, the AlSiMg alloy was used. To validate the choice of material, an analysis was made with the finite element method. The study process is identical to that performed on the steel frame. The same conditions applied to constraints and loads. The resulting convergence graph is presented in Fig. 7.12.

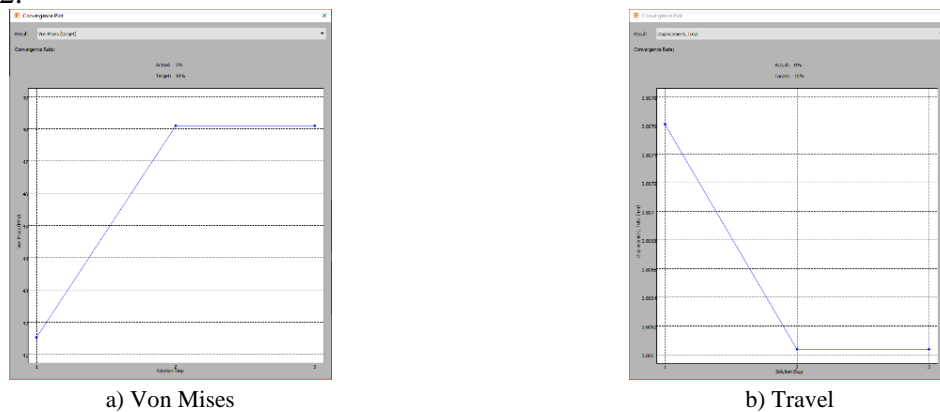


**Fig. 7.12** - Convergence diagram for the study of AlSiMg stress

The test results show that the AlSiMg alloy is strong enough to withstand the load of 1200 N with a maximum deformation of 0.80 mm and a minimum safety factor of 5.78, which is slightly above the minimum safety factor for this type of application, presented in Fig. 7.13. The weight of the frame was reduced to 3.69 Kg, reaching the weight target.

The program generates a final discretization, which shows the essential areas that cannot be modified and the areas from which the amount of material can be reduced, and it can be superimposed over the 3D model, in order to optimize it.

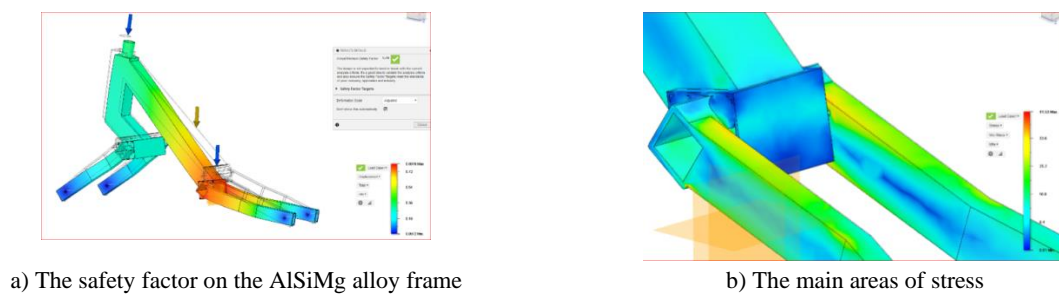


**Fig. 7.13** - Simulation results

Subsequently, the 3D model will be modified according to the results of the optimization process.

The new 3D model, optimized, can be validated by performing a new series of force loading studies, which will check the safety factors of tension, displacement and safety factor to determine whether the part is resistant to handling applied loads.

The result is good enough for the target weight of the final product, but an attempt was made to reduce the weight of the frame even more, to make it more efficient and easier to use. Topological optimization was performed by applying the same rules as for the steel frame. The results are presented in Fig. 7.14.

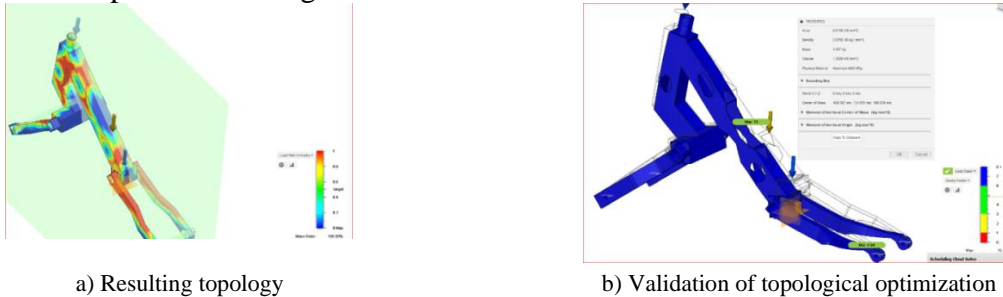


**Fig. 7.14.** - Topological optimization results for the AlSiMg framework

The topology generated by the program on the new model suggests the asymmetric removal of the material from the central axis. The new structure generated is 3.38 Kg lighter than the old one, 3.69 Kg.

The new topology was superimposed over the 3D model in order to remove the material from the areas suggested by the program.

The new generated form was subjected to a new static force loading study in order to test the results of the optimization process.

For this study the same parameters used in the static study of the initial concept were used

This study also focused on testing several types of material usually used in such structures, in order to propose construction variants depending on the type of use of the product or the weight of the user.

In order to perform this study, a convergence analysis of the size of the discretization element, the relative number of nodes required and the deformation of the material on the structure model was performed. The parabolic discretization element was used. The Fusion simulation module uses the standard size for the 130 mm discretization element. For this analysis, element values between 330 mm and 80 mm were taken.

The materials used in this study are AISI 1061 Steel and AlSiMg. The loading of the structure was done by loading the handlebars and the pedal area, with a force of 400 and 800 N directed downwards, simulating the force with which the user's weight is pressed. In order to constrain the structure, the fixing elements were used, through which it will be mounted in the frame.

In order to obtain an optimal safety factor and to be able to validate the simulation results, for this structure, the properties of the chosen material and the type of construction were taken into account.

## **Chapter 8. Conclusions, own contributions, development perspectives**

### **8.1. conclusions**

Starting from the instrumentalization of the life cycle of a product, this paper presents the stages of conception and realization of a new product. The succession of these stages was implemented in order to achieve a viable solution, of the tricycle type, to the transport problems in the urban environment. Following the analysis of the designed vehicle regarding the parameters during use, the optimization stages were illustrated by prototypes providing the necessary information taking into account the issues of stability, maneuverability and ergonomics.

The prototypes presented offer the same degree of freedom as that of a motorcycle, a positive and recognizable aspect for the user, which gives him the opportunity to get acquainted with the product faster.

The tricycle, on the other hand, offers higher safety than a conventional motorcycle, offering higher stability due to the three wheels. Also the noise level is very low, not having a heat engine.

By developing and implementing the tilt and damping system, the tricycle offers a high degree of user comfort, an aspect that is lacking in other similar means of alternative transport.

Regarding the stability of the vehicle during cornering, it was observed during the tests that the tilt system helps to counteract the centrifugal force present at the cornering. This compensation is reflected both in the comfort of the passengers and in the stability of the vehicle.

The product meets the objectives in terms of user experience, namely: comfort, safety, economy and mobility. These aspects have been the basis for the development of the tricycle and also promote the concept of intelligent ecological transport, through the decongestion capacity of urban areas once implemented.

The ultimate goal of this research was not only conceptual, but involved the concrete development of a foldable electric tricycle, easy to use, but robust, able to provide a comfortable driving experience on every type of road. The main contributions are the design of the tricycle structure together with the folding mechanism, the development of a frame-specific suspension system using elastic damping elements and the measurement of stress values in several key locations on the tricycle frame using tensometric transducers. These studies led to the realization of physical prototypes subsequently analyzed and compared, thus establishing the optimal variant of geometry and construction to be further improved, based on measurements made during this research.

The proposed, designed concept is a solution that aims to solve, even partially, the problems reported in the first chapter of the paper, in accordance with objective 1 of the paper.

- The concept works, in this context, providing a suitable vehicle for travel in urban areas and beyond, independent and easy use, providing a high degree of mobility, thus meeting objective 4 of the paper.
- The proposed system brings extra comfort for users who use alternative transport.
- The folding system brings a positive aspect, allowing easier ascent and descent of the tricycle in different storage spaces thus fulfilling objective 4 of the paper.
- The proposed concept offers a high level of safety for users due to the damping and tilting system developed, in accordance with objective 6 of the paper.

- The paper also aimed to make practical prototypes in order to understand and analyze existing experiences and user needs, with a low initial production cost. The design of the assembly can be analyzed faster, allowing experimentation, with several iterations, in a relatively short time. The purpose of prototyping is to show the capabilities of a product by building an inexpensive series so that designers are able to get quick feedback that can meet user requirements. Thus, the prototypes made in the paper show that:

- the proposed solution for the frame / folding system is a viable one;
- the fastening and fixing systems allow the interchangeability of the component elements (objective 5);
- the use of standardized elements (rectangular profiles, motors, batteries, wheels) reduces costs (objective 5);
- maintenance and replacement of obsolete items is easier if standardized items are used (Objective 5);
- ergonomic considerations and chosen proportions determine the shape and dimensions of the components (Objective 9);

Studies have led to the conclusion that this proposed concept works and will withstand the demands that arise during operation.

Component optimization was done using the Auto Works and CAD Fusion 360 programs from AutoDesk in the “Simulation / Shape Optimization” simulation module. The optimization process is similar to that of the force study considering the constraint data (material, fixing system).

The following can be stated:

- The optimization process was efficient;
- The constructive approach in order to stiffen according to the topology suggested by the program led to form optimizations that correspond to the proposed objectives (objectives 3, 4, 7,11).

The 3D model optimized by the topology suggested by the program withstands maximum values of the demands during operation.



**Fig. 8.1** - Aggregate electric tricycle with agricultural equipment [68]

## 8.2. Own contributions

- Synthesizing the theoretical approaches, investigation methods and original practical achievements we obtain 14 main elements as follows
- Proposed design for an original variant of an electric vehicle (objective 2, objective 5, objective 6, objective 7).
- Design a compact, easy-to-use, space-saving product (Objective 2, Objective 3, Objective 4).
- Simulating the behavior of virtual prototypes using successive programs in SolidWorks and AutoDesk Fusion 360 programs (goal 7, goal 9)



- Conception and validation of a solution to increase the stability of the tricycle using a ROSTA type suspension / damping system as a tilt mechanism.
- Improving overall behavior by choosing an appropriate suspension size.
- The introduction of a folding system that brings an innovative element, allowing easier ascent and descent of the tricycle in different storage spaces thus fulfilling objective 4 of the paper.
- Realization of elements with original shape from the composition of the product, articulation and inclination system, frame geometry, fairing.
- Practical realization of some variants of the product that can be adapted for different types of land, urban but also rural environment (objective 2, objective 3). The operation of these variants is easy and complies with the rules in force (objective 4).
- Inclusion in the final solution of some standardized elements (wheels, metal profiles, batteries, motors) objective 5, objective 7 which ensures the optimization of the price-quality ratio.
- Validation of the final prototype as a simple, proportionate construction that respects the conditions of ergonomics (objective 11)
- The product was protected at OSIM by registration of patent application A 00625 of 04.10.2019 [69]
- The invention was awarded at the “UGAL INVENT” Innovation and Research show, Galați 2019
  - Diploma and Gold Medal
  - Diploma of Excellence "Justin Capra"
  - Diploma of Excellence INMA Bucharest
- The product was awarded by the Dan Voiculescu Foundation at the Bucharest Motor Show (SAB 2017) on the occasion of participating in the scholarship competition of the show
- The product was disseminated at the International Symposium ISB-INMA TEH Bucharest 2019

### **8.3. Development perspectives**

Further research will focus on establishing an optimal manufacturing architecture for the new product described in this thesis. At the beginning, a modeling of the preliminary manufacturing architecture will be performed with the parameterization of the working points, of the transport and transfer systems and of the storage systems. The trajectories that the material flows of semi-finished products, parts and tools will follow within these architectures will be established. The material flows of semi-finished parts and tools in this pre-fabricated architecture will be simulated.

Based on the diagnosis obtained from the reports that monitor the performance parameters of the studied architecture, the flow concentrators will be identified, where it is slowed down or even blocked. Two solutions for the elimination of these concentrators will be considered. Functional remodeling enhances the performance of the manufacturing architecture through changes in the location of structural elements, the order of operations, the operating parameters of the structural elements but does not eliminate or introduce structural elements in the manufacturing architecture.

Technological remodeling also allows changes in the manufacturing architecture by introducing or removing structural elements (work points, transfer and transport systems, storage systems).

After the technological or functional remodeling, the material flows will be simulated again to monitor the increase of the performance parameters of the manufacturing architecture.

The last stage is the necessary economic validation if we used a technological remodeling that involves an investment in modifying the manufacturing architecture. The financial value resulting from the enhancement of the performance indicators optimized by remodeling must be greater than the value of the investment required to modify the architecture.

If in the thesis the researches were focused on the assisted design module that generates the virtual prototype of the product, further the researches will be focused on the MFM modules that generate the virtual prototype of the manufacturing architecture. By simulating the material flows at the level of this virtual prototype, diagnoses will be obtained every time changes in the manufacturing architecture occur as a result of the introduction of new products in production. The virtual prototype of the manufacturing architecture will be the main optimization tool when the new manufacturing architecture needs to be finalized and validated.

A broader perspective considers optimizing the structure of the product by using composite materials for the manufacture of the frame and auxiliary components in order to reduce its weight.

The product will be modified to extend its use to the agricultural machinery industry, offering the possibility to connect different specific aggregates through modular integration (Fig. 8.1) [70], [69].

Another direction of development is specific to the leisure industry by adapting the product for various electric motor sports competitions. The tricycle can also be adapted for use by people with locomotor disabilities.

One of the aspects that could be added in the future to increase comfort would be to build a user support point, for example a chair, a saddle.

## Bibliography

- [1] Noon Matthew, "urbact.eu," EVUE electric vehicles in Europe, October 2012. [Interactive]. Available: [https://urbact.eu/sites/default/files/import/Projects/EVUE/documents\\_media/EVUE\\_Final\\_Report\\_October\\_2012-RO\\_ok.pdf](https://urbact.eu/sites/default/files/import/Projects/EVUE/documents_media/EVUE_Final_Report_October_2012-RO_ok.pdf). [Accessed 20 03 2016].
- [2] Bărbulescu, Ovidiu, „profit.ro,” Confirmation of the new state aid scheme: Subsidy for companies that invest in electric charging stations, June 12, 2019. [Interactive]. Available: <https://www.profit.ro/taxe-si-consultanta/confirmarea-noua-schema-de-ajutor-de-stat-subventie-pentru-firmele-care-investesc-in-statii-de-incarcare- power-19,030,452>. [Accessed June 12, 2019].
- [3] Court of Auditors, "europa.eu," Renewable Energy for Sustainable Rural Development, May 2018. [Interactive]. Available: <https://op.europa.eu/webpub/eca/special-reports/renewable-energy-5-2018/ro/>. [Accessed April 18, 2019].
- [4] Niemann, J., Westkämper, E., „The paradigm of product life cycle management - Continuous planning, operation and evaluation of manufacturing systems „,” International conference of integrated engineering, Timisoara, Romania „, pp. P.29-30, , 2005.
- [5] DRAGHICI, George; SAVII, George & DRAGHICI, Anca, “Platform for collaborative product and processes development,” The 18th international dam symposium, pp. 24-27, October 2007.
- [6] CIMdata, “Product Lifecycle Management (PLM) Definition,” pp. <https://www.cimdata.com/en/resources/about-plm>.
- [7] Don S., “Managing products and portfolios with PLM key initiative overview,” April 09, 2014.
- [8] IBM, “Business process management for automotive end of life processes,” pp. <http://www.redbooks.ibm.com/redpapers/pdfs/redp4451.pdf>, 03 September 2008.
- [9] Stark J., “PLM: 21st century paradigm for product realization, springer-verlag „,” 2004.
- [10] Cotet, CE, Popescu, D., Popa, CL, „Management of material flows in industrial engineering,” POLITEHNICA PRESS Publishing House, p. 153, 2014.
- [11] Cotet CE, Popescu, D., „Material Flow Management in Industrial Engineering, in Encyclopedia of Information Science and Technology, Category: Industrial Engineering, Third Edition, Editor Mehdi Khosrow-Pour „,” Published in the United States of A, 2014.
- [12] Tom tom, “tomtom.com,” [Interactive]. Available: [https://www.tomtom.com/en\\_gb/traffic-index/bucharest-traffic#statistics](https://www.tomtom.com/en_gb/traffic-index/bucharest-traffic#statistics). [Accessed 23 May 2019].
- [13] APH, “Dockless Electric Scooter Study,” April 2019. [Interactive]. Available: [https://www.austintexas.gov/sites/default/files/files/Health/Epidemiology/https://www.austintexas.gov/sites/default/files/files/Health/Epidemiology/APH\\_Dockless\\_Electric\\_Scooter\\_Study\\_5-2-19.pdf\\_Dockless\\_Electric\\_Scooter\\_Study\\_5-2-19.pdf](https://www.austintexas.gov/sites/default/files/files/Health/Epidemiology/https://www.austintexas.gov/sites/default/files/files/Health/Epidemiology/APH_Dockless_Electric_Scooter_Study_5-2-19.pdf_Dockless_Electric_Scooter_Study_5-2-19.pdf). [Accessed 16 August 2019].
- [14] Scrigroup, “scrigroup,” April 26, 2006. [Interactive]. Available: <http://www.scrigroup.com/tehnologie/electronica-electricitate/Triciclete-electrice21787.php>. [Accessed November 2, 2015].
- [15] CH Thomas, “jetrike.com,” November 9, 2007. [Interactive]. Available: <http://www.jetrike.com/tadpole-or-delta.html>. [Accessed 22 November 2015].
- [16] H. Fell, “sheldonbrown.com,” December 2008. [Interactive]. Available: [https://www.sheldonbrown.com/gloss\\_tadpole.html#tadpole](https://www.sheldonbrown.com/gloss_tadpole.html#tadpole). [Accessed January 6, 2016].
- [17] Riley, Robert Q., “rqriley.com,” [Interactive]. Available: <https://rqriley.com/the-dynamic-stability-of-three-wheeled->

- vehicles-in-automotive-type-applications/. [Accessed April 17, 2017].
- [18] Amin Saeedi, Reza Kazemi, "Stability of Three-Wheeled Vehicles with and without Control System," International Journal of Automotive Engineering, Vol. 1 of 2 Vol. 3, no. Number 1, March 2013.
- [19] THECOOLIST, "thecoolist," [Interactive]. Available: <https://www.thecoolist.com/johammer-j1-electric-motorcycle/>. [Accessed 16 MAY 2019].
- [20] Acton, "actonglobal.com," 2013. [Interactive]. Available: <https://www.actonglobal.com/products/m-scooter>. [Accessed 5 October 2015].
- [21] Kroonen, CR van den Brink and HM, "DVC - The banking technology driving the carver vehicle class," AVEC '04, 2004.
- [22] Qugo, "qugo.nl," 2016. [Interactive]. Available: [://www.qugo.nl/nl/de-qugo](http://www.qugo.nl/nl/de-qugo). [Accessed November 20, 2016].
- [2. 3] John Tolhurst, "www.academia.edu," Tilting Tricycle Suspension Arms Assembly, [Interactive]. Available: [https://www.academia.edu/7666065/Tilting\\_Tricycle\\_Suspension\\_Arms\\_Assembly?email\\_work\\_card=reading-history](https://www.academia.edu/7666065/Tilting_Tricycle_Suspension_Arms_Assembly?email_work_card=reading-history). [Accessed 23 June 2019].
- [24] Farmer C, "Effect of electronic stability control on automobile crash risk," Traffic Inj Prev., Vol. 4, no. 5, pp. 317-25, 2004.
- [25] Foale, Tony, "motochassis.com," [Interactive]. Available: <https://motochassis.com/Articles/Balance/BALANCE.htm>. [Accessed 03 June 2017].
- [26] Rosta, "rosta.ch," [Interactive]. Available: <https://www.rosta.ch/en/about-us/history/>. [Accessed January 15, 2016].
- [27] Raluca Cardei, Petru Vergil, Muraru Munteanu Alexandru Sfiru, "researchgate.net," January 2010. [Interactive]. Available: [https://www.researchgate.net/publication/313478659\\_ELEMENTARY\\_NON-LINEAR\\_WITH\\_LINEAR\\_DAMPING\\_MATHEMATICAL\\_MODEL\\_FOR\\_NEIDHART\\_SUSPENSION\\_MODEL\\_MATEMATIC\\_ELEMENTAR\\_PENTRU\\_SUSPIZIN](https://www.researchgate.net/publication/313478659_ELEMENTARY_NON-LINEAR_WITH_LINEAR_DAMPING_MATHEMATICAL_MODEL_FOR_NEIDHART_SUSPENSION_MODEL_MATEMATIC_ELEMENTAR_PENTRU_SUSPIZIN). [Accessed 18 October 2015].
- [28] Rosta, "rosta.ch," [Interactive]. Available: <https://www.rosta.ch/en/products/rubber-suspension-technology/>. [Accessed 12 May 2016].
- [29] Theuniversalgroup, "theuniversalgroup.com," February 2018. [Interactive]. Available: <http://www.theuniversalgroup.com/wp-content/uploads/2018/03/P10-Flexiride-brochure.pdf>. [Accessed 12 July 2018].
- [30] yikebike, "yikebike.com," October 13, 2013. [Interactive]. Available: <http://www.yikebike.com/model-v/>. [Accessed 6 February 2015].
- [31] ecomobilitate, "ecomobilitate.ro," January 9, 2014. [Interactive]. Available: [https://ecomobilitate.ro/VT3#page\\_artdet\\_tabs](https://ecomobilitate.ro/VT3#page_artdet_tabs). [Accessed March 19, 2016].
- [32] P. Ridden, "newatlas.com/," June 5, 2018. [Interactive]. Available: <https://newatlas.com/ridroid-canguro/55328/>. [Accessed 03 August 2018].
- [33] J. Glide, "yamaha-motor.com," November 9, 2018. [Interactive]. Available: <https://global.yamaha-motor.com/news/2018/1109/ces2019-tritown.html>. [Accessed November 10, 2018].
- [34] s3tr, "s3tr.hr," November 23, 2013. [Interactive]. Available: <https://www.s3tr.hr/#specifications>. [Accessed March 7, 2016].
- [35] Camilo Parra-Palacio, Gilberto Osorio-Gómez, Ricardo Mejía-Gutiérrez, "Approach to industrialization of academic projects," Innovation in Engineering, Technology and Education for Competitiveness and Prosperity, Cancun,

- Mexico., Pp. 14-16, 2013.
- [36] Hans Pacejka, in *Tire and vehicle dynamics*, Elsevier, 2006.
- [37] Campian, Horațiu, “freerider.ro,” November 10, 2016. [Interactive]. Available: <https://freerider.ro/noutati/nexo-inca-o-idee-de-anvelopa-fara-aer-113850.html>. [Accessed November 10, 2016].
- [38] Jack Oortwijnon, “bike-eu.com,” January 26, 2017. [Interactive]. Available: [https://www.bike-eu.com/home/nieuws/2017/01/accell-launches-e-bike-motor-with-integrated-5-speed-gear-hub-10128755?\\_ga=2.216709462.1731975913.1567894472-2015621871.1567894472](https://www.bike-eu.com/home/nieuws/2017/01/accell-launches-e-bike-motor-with-integrated-5-speed-gear-hub-10128755?_ga=2.216709462.1731975913.1567894472-2015621871.1567894472). [Accessed 22 February 2018].
- [39] Yi-Tsung WuHok-Sum Horace LukeJui Sheng Huang Matthew Whiting TaylorHuang-Cheng Hung, “Apparatus, method and article for a power storage device compartment,” pp. <https://patentimages.storage.googleapis.com/ed/97/14/ef2953c57ad203/US9424697.pdf>, 23 August 2016.
- [40] Makeagif, “Regenerative Braking,” pp. <https://makeagif.com/gif/volkswagen-regenerative-braking-energy-recovery-in-electric-drives-qGfWM->.
- [41] Wikipedia, “Regenerative Braking,” p. [https://ro.wikipedia.org/wiki/Fr%C3%A2nare\\_regenerativ%C4%83](https://ro.wikipedia.org/wiki/Fr%C3%A2nare_regenerativ%C4%83).
- [42] Lambros Laios, John Giannatsis, “Ergonomic evaluation and redesign of children bicycles based on anthropometric data,” *Applied Ergonomics*, vol 41, pp. 428-435, 2010.
- [43] Dragos Mitroi, “freerider.ro,” October 26, 2018. [Interactive]. Available: <https://freerider.ro/mag/componente-ergonomice-cum-sa-ti-faci-bicicleta-mai-comoda-141061.html>. [Accessed November 14, 2018].
- [44] A. Claudiu, “Science and Technology,” *Greeny electric tricycle*, pp. 29-31, 12 January 2012.
- [45] BSD Tripp, “Rapid Prototyping: An Alternative Instructional Design Strategy,” *Educational Techonlogy Research and Development*, pp. 31-44, 1990.
- [46] Wang, YF, Lei XY, Zhang, GL, Li, SJ, Qian, HH, Xu YS, “Design of Dual-spring Shock Absorption System for Outdoor AG,” 2017 IEEE International Conference On Information And Automation, vol 345, no. . 47, pp. 159-164, 2017.
- [47] Spiroiu MA., „Railway vehicle pneumatic rubber suspension modeling and analysis,” *Materiale Plastice Journal*, vol. 55, nr. 1, pp. 24-27, 2018.
- [48] Nielens H., Lejeune T., “Bicycle shock absorption systems and energy expended by the cyclist.” *Sports Medicine Journal*, vol 34, no. 2, pp. 71-80, 2004.
- [49] Nielens H., Lejeune TM, “Energy cost of riding bicycles with shock absorption systems on a flat surface.” *International Journal of Sports Medicine*, vol 22, no. 6, pp. 400-404, 2001.
- [50] Neto FPL., Santos MB, „A Procedure for the Parametric Identification of Viscoelastic Dampers Accounting for Preload,” *Journal of the Brazilian Society of Mechanical Sciences and Engineering*, vol. 2, no. 34, pp. 213-218, 2012.
- [51] Albert Suvac, Aurel Solomon, Cristian-Gabriel Alionte, Liviu-Marian Ungur, “Design and analysis of an efficient shock absorption system,” 2019.
- [52] Yafeng Wang, Xiangyu Lei, Guilin Zhang, Shuaijun Li, Huihuan Qian, Yangsheng Xu, “Designing the Double Arc Shock Absorber System for Outdoor AGV,” at *IEEE Xplore*, Macau, China, October 23, 2017.
- [53] Buburuz, Bogdan, „vocea.biz,” *Greeny*, the electric scooter “made in Romania” that wants to be an alternative to the car in the urban agglomeration, pp. <https://vocea.biz/social/2017/apr/02/greeny-electric-scooter-made-in-romania-what-is-wanted-an-alternative-to-car-in-urban-agglomeration/>, 02 april 2017.

- [54] Leilei Zhao, Yuewei Yu, Changcheng Zhou, Fuxing Yang, "Modeling and validation of the rubber spring suspension for off-road vehicles," *Journal of Vibration and Control*, vol. 24, no. 18, pp. 4110-4121, July 10, 2017.
- [55] Diaconescu, Radu, "freerider.ro," January 21, 2013. [Interactive]. Available: <https://www.freerider.ro/mag/cum-functioneaza-o-furca-cu-suspensie-43158.html>. [Accessed December 9, 2014].
- [56] Radu Diaconescu, "How does a fork with suspension work," pp. <https://freerider.ro/mag/cum-functioneaza-o-furca-cu-suspensie-43158>, January 21, 2013.
- [57] utcluj, „sim.utcluj.ro,” [Interactive]. Available: <http://www.sim.utcluj.ro/stm/download/sim/Curs%202.pdf>. [Accessed October 15, 2018].
- [58] NOLAND, DAVID, "https://www.greencarreports.com/," Tesla Model S Aluminum Body, January 15, 2015. [Interactive]. Available: [https://www.greencarreports.com/news/1096220\\_tesla-model-s-aluminum-body-why-repair-costs-are-higher?fbclid=IwAR0S2CMTtd\\_-icgkpILQ8cpcuDrxgRif4EuRMBKY4e](https://www.greencarreports.com/news/1096220_tesla-model-s-aluminum-body-why-repair-costs-are-higher?fbclid=IwAR0S2CMTtd_-icgkpILQ8cpcuDrxgRif4EuRMBKY4e). [Accessed 23 May 2017].
- [59] PS Theocaris, M. Buga, C. Burrada, M. Baltanaoiu, I. Constantinescu, D. Horbaniuc, N. Ilescu, DR Mocanu, M. Modiga, L. Nailescu, I Pascariu, VL. Popovici, M, Tripa, Analysis experimental of the tensions the theoretical bases of the tensometric methods and the practical indications regarding their use, Bucharest: Bucharest Technical Publishing House, 1977.
- [60] PS Theocaris, C. Atanasiu, L. BOLEANTU, M. BUGA, C. BURRADA, I. CONSTANTINESCU, N.ILIESCU, DR MOCANU, M. MODIGA, I PASTRAV, M TEODORU, Experimental analysis of stresses theoretical bases of tensometric methods and practical indications regarding their use, BUCHAREST: TECHNICAL PUBLISHING HOUSE BUCHAREST, 1976.
- [61] DAQ systems with LabVIEW, "Connecting sensors and signals at the DAQ module," Strain gauges, pp. <https://sites.google.com/site/sistemedaq/cuprins/connect-sensors-and-signals-to-a-daq> -Deva / 5-strain-gages / principles.
- [62] Valentina POMAZAN, Alexandru POMAZAN, "AESTHETIC SOLUTIONS FOR REINFORCEMENTS," *AGIR Bulletin*, 2015.
- [63] Aranda B., Lasch C., Tooling, New York: Princeton Architectural Press, 2006 ..
- [64] Bollobas B., Riordan O., Percolation Cambridge, Cambridge University Press: Cambridge, 2006.
- [65] Marco Cavazzuti, Dario Costi, Andrea Baldini, Patrizio Moruzzi, „Automotive Chassis Topology Optimization: a Comparison Between Spider and Coup´e Designs,” *Proceedings of the World Congress on Engineering 2011 Vol III WCE 2011*, July 6 - 8, 2011, London, UK, 2011.
- [66] Albert Mihai Suvac Lucian CUCU, Radu Constantin PARPALA, Cosmin LAZAR, "Shape Optimization Through Parametric Design Methods Using Cad Software," *Research and Science Today*, 2017.
- [67] Mihai, Suvac Albert; Lucian, Cuckoo; Radu, Parpala; Cosmin, Lazar, "Shape optimization through parametric design methods using CAD software," *Research and science today*, vol. 2, no. 2285-9632, 2017.
- [68] Suvac AM, Ganea-Christu I., „Electrically powered tricycle aggregated with agricultural Equipment. Volume,” *ISB INMA TEH 2019*, no. ISSN 2344-4118, pp. 533-538, 2019.
- [69] Suvac AM, Ganea-Christu I., "Electrically powered tricycle to be aggregated with small agricultural equipment," no. A-00625, 2019.
- [70] Suvac AM, Ganea CI, „Electrically powered tricycle aggregated with agricultural Equipment. Volume,” *ISB INMA TEH 2019*, no. ISSN 2344-4118, pp. 533-538, 2019.